Order Number 9000686

An analysis of ARQ and hybrid FEC-ARQ transmission over a meteor burst channel

Djuknic, Goran M., Ph.D.

City University of New York, 1989

U·M·I
300 N. Zeeb Rd.
Ann Arbor, MI 48106

A

AN ANALYSIS OF ARQ AND HYBRID FEC-ARQ TRANSMISSION OVER A METEOR BURST CHANNEL

by

GORAN DJUKNIC

A dissertation submitted to the Graduate Faculty in Engineering in partial fulfillment of the requirements for the degree of Doctor of Philosophy, The City University of New York

1989

This manuscript has been read and accepted for the Graduate Faculty in Engineering in satisfaction of the dissertation requirement for the degree of Doctor of Philosophy.

4/25/89
Date

Chair of Examining Committee

4/27/89
Date

Jacques E. Bouvenuste
Executive Officer

Prof. Joseph Barba

Prof. Sorin Davidovici

Prof. Eliphaz Hibshoosh

Prof. Tarek Saadawi

Supervisory Committee

The City University of New York

Abstract

AN ANALYSIS OF ARQ AND HYBRID FEC-ARQ TRANSMISSION OVER A METEOR BURST CHANNEL

by

Goran Djuknic

Adviser: Professor Donald L. Schilling

Meteor burst channel is an intermittent channel, the time of its appearance and its duration are random variables. It is described in terms of stochastic parameters: meteor trail arrivals, electron line densities of underdense and overdense trails, and underdense power decay constant.

Two ARQ strategies, for point-to-point data transmission, were considered: "stop-and-wait", where one data packet is transmitted per burst, and "selective-repeat", where the entire burst duration is used for information transmission. In addition, ARQ is combined with forward error-correction, leading to a hybrid FEC-ARQ scheme. Using the probabilistic parameters, expressions were derived for ARQ system performance characteristics: throughput rate,

message waiting time, and the probability of successful message delivery within some specified time. Performance measures are functions of communication system parameters, transmission protocol, packet size and transmission data rate. It is shown that in a stop-and-wait protocol there always exists an optimum packet size that maximizes the throughput, when data rate is kept fixed, and an optimum data rate that minimizes the message waiting time, when packet size is fixed. It is also shown that in both protocols coded transmission yields higher throughput, lower message waiting time, and increased probability of correct message reception, as compared to uncoded transmission, but only when code rate approaches to 1. The coding employed was rate-1/n and k/n convolutional, with BPSK modulation.

We also estimated the channel duty cycle and channel capacity, the latter when meteor burst channel is regarded as a Gaussian channel and a binary-symmetric channel. They are functions of random channel parameters and communication system characteristics, and independent of the transmission protocol.

ACKNOWLEDGEMENT

It was a privilege to work with Professor Donald Schilling. He introduced me to this research area, his words of encouragement and his illuminating insight were invaluable in completing the work.

Innumerable discussions and deliberations with Professor Eli Hibshoosh, and his experience in this topic, helped in defining and achieving the research goals. Professors Joe Barba, Tarek Saadawi, and Sorin Davidovici were more than helpful with their remarks.

I dedicate this work to:

My parents, whose faith in my capabilities gave me strength to always strive for the better, and

My dear friends of many years, Dr. Dragana Brzakovic and Dr. Danilo Golijanin, who made that road a more pleasant experience.

Table of Contents

List of Illustrations

1. INTRODUCTION

Meteor burst is a useful technique for low data rate digital communications at ranges from 800 to 2000 kilometers. There is still some controversy about the usefulness of meteor burst as the range decreases below 400 km, but several experiments have shown that communication is possible if the antenna patterns are designed properly [39] [48].

Billions of meteors of different sizes enter the earth's atmosphere each day. They are trapped by earth's gravitational field while orbiting around the sun. Here, the term "meteor" is applied only to those cosmic particles entering the atmosphere that are completely burned by frictional heating. Their masses range from 10^{-7} to 10^{3} grams, and dimensions from 40 μm to 8 cm [50].

Two classes of meteors are usually distinguished. The "shower" meteors are groups of particles moving at the same velocities in pretty well-defined orbits around the sun. Their orbits intersect the orbit of the earth at a specific time each year, and then they appear to be coming from one

"radiant" point in the sky.

"Sporadic" meteors are of main interest in radio communication, since shower meteors account for only a small fraction of all meteors. Radiant points for sporadic meteors are randomly, but not uniformly, distributed over the sky. For the most part, they are concentrated toward the ecliptic plane. Their orbits are also nonuniformly distributed along the earth's orbit, and thus produce the maximum incidence of meteors in July, and the minimum in February.

The numbers of sporadic meteors are inversely proportional to their respective masses, in such a way that there are approximately equal total masses of each size of particle. Ten times as many particles of mass, say, 10^{-4} g appear as of mass of 10^{-3} g.

Most observations indicate that the meteors are members of the solar system. Their velocities in approaching the earth range from 11.3 to 72 km/sec. Those are the first and the second cosmic speeds, escape velocities for the particle to leave the earth and solar system, respectively.

The earliest report of improved radio reception due to meteor showers is from 1931 [43], but the correlation between radio signals and individual meteor trails was not clearly established until 1946 [24]. The experimental basis for future theoretical work was established by VHF ionospheric scatter observations started in 1951 [3].

The impetus for the development of meteor burst communication systems was provided by the expression for channel capacity

$$C = S_1^{\alpha}\ \rho_t^{-\alpha/2}\ N^{-\alpha}\ B^{1-\alpha/2}\ ,$$

derived by Sugar [50], and Montgomery and Sugar [37]. The messages are sent only if signal-to-noise values exceed threshold value ρ_t. N is the noise power spectral density, B is the system bandwidth, and S_1 is a positive constant.

Early measurements indicated that $\alpha = 1.2$ was typical. Recent data show that its value may be closer to 1.6 for underdense trails [58]. The importance of this result lies

in the fact that for $0 \leq \alpha < 2$ the channel capacity increases with the signaling bandwidth, making the communication feasible.

The frequency range for radio transmission using meteor burst is a lower VHF range, from 30 to 110 MHz. The lower limit is set as to be above the maximum usable frequency for ionospheric reflections, and the upper limit is due to equipment sensitivity limitations.

The signal loss in radio transmission over a meteor burst channel is relatively high. A communication system with 50 MHz carrier, transmitter power of 2 kW and 1300 km distance between stations, will encounter 170 dB system loss. Meteor scatter loss is is about 80 dB, and 90 dB is associated with the length of a transmission path.

The communication is intermittent, and information message is transmitted only when a pilot signal from receiver is sensed, indicating the presence of a meteor channel. When the channel is not present, the information is being stored in the transmitter buffer memory. It waits there for the opening of the channel, when it is sent in

a burst manner.

One of the earliest attempts to use the forward-scattered radio signals from ionized trails of individual meteors, in order to establish long-range VHF communication, was the Canadian JANET Meteor Burst Communication System [12] [16]. The experimental test link, 600 miles long, was established between Toronto and Port Arthur in the summer of 1955. It demonstrated the feasibility of reliable communication for teletype transmission, at information rate of up to 60 words per minute.

Relying on experiences from the JANET system and incorporating ARQ and diversity reception techniques, a new meteor burst communication system COMET was developed in 1966. Its role was to make efficient use of meteor trail reflections for telegraph transmission in the VHF band, over distances of up to 2000 km. It was tested on a 1000 km path between Netherlands and the South of France [4]. The information was transmitted at an instantaneous rate of 2000 bauds, and the flow of information was based on an error-detection scheme with automatic-repeat-request.

Those early experimental successes were followed by theoretical advances in statistical model development, and theoretical assessments of performance characteristics. In a comprehensive survey of the meteor burst channel, Oetting presented the methodology for design and analysis of meteor burst communication systems [41], two main performance characteristics were estimated: throughput and probability of completing a message during an arbitrary observation time. Meteor trail arrival was modeled as a Poisson process. Average interval between bursts was calculated according to the reference method, where the meteoric arrival rate of a known test link is scaled by a number of factors which compensate for differences between the link of interest and the test link. This basic approach projects the mean time between trail arrivals (underdense and overdense combined,) as

$$t_I = t_{IC} \left(\frac{G_T}{G_{TC}} \frac{R_C}{R} \frac{G_R}{G_{RC}} \frac{P_T}{P_{TC}} \right)^{-0.6} \left(\frac{f}{f_C} \right)^{2.4}$$

where the subscript 'C' denotes the parameters of a reference COMET system [4]. Yearly averages for t_{IC} are 4 seconds in the early morning hours, and 20 seconds in the

late afternoon hours. Recent experimental data suggest that more precise models are needed for better prediction of real physical situations [58]. Thus, Oetting's estimates of the waiting time to receive a message with required degree of confidence are somewhat on the pessimistic side. In his work, no coding of information packets was considered.

Using the Sugar's probabilistic model, Weitzen et al. estimated the capacity of the meteor burst channel, by averaging the random received power from a trail over instantaneous data rate and electron line density [55]. Under ideal conditions, in which a transmitter is capable of measuring signal strength and multipath spread and instantaneously match its information transfer rate to the channel conditions, while maintaining a given error rate, the average daily capacity is determined to be about 14 kbits/sec. That showed space for improvement over contemporary constant rate systems, that achieved average throughput on the order of 150 bits/sec.

Brown has developed a computer model of meteor burst propagation to support the design of meteor burst commu-

nication systems [8]. It includes all major physical processes at work in a meteor burst link, except for an overdense trail model, and is based mostly on data from the experimental link between Netherlands and the south of France [4]. Experimental and calculated data are compared for duty cycle values in relation to carrier frequency, path length, antenna system, time of day, and geographical latitude of a link. Throughput is related to transmission rate, and message delay to message length and data rate. Data are shown to agree at two widely separated frequencies on one experimental link. The main conclusion is that substantial improvements can be obtained by optimizing antenna patterns, on a link by link basis.

Abel used classical equations for received power to derive performance bounds for a meteor burst communication medium [1]. They give the maximum number of bits that can be transmitted during a single burst, using either an optimum constant bit rate or a continuously varying bit rate. The latter technique was shown to have the advantage over the first one, achieving two to three times higher maximum number of bits per given burst. Bits per burst maxima also vary with link parameters, great circle distance

between terminals and wavelength, as well as with trail electron line density. In addition, the optimum constant bit rate bound was used to estimate long-term average bit rate and its relation to changes in electron line density.

As a continuation of Oetting's work, Milstein et al. analyzed the expected throughput and the probability of receiving a given message correctly during the observation time, under two transmission protocols [36]. In the first protocol, the entire duration of a burst was known to the transmitter, and in the second only the starting times of each meteor burst were known. The information packet was protected by a Reed-Solomon block code, and performance of a communication system was evaluated for different code rates and signal-to-noise ratios. Throughput was calculated for various packet sizes, showing that there is an optimum packet size in case of the second protocol. In a probabilistic model used, trail arrivals are governed by a Poisson random process, and burst duration d_b follows exponential probability density

$$f(d_b) = \frac{1}{T_L} \exp\left(-\frac{d_b}{T_L}\right),$$

where T_L is the average burst length. In our work, more complex burst duration statistics is used, Eq. (2.1.4-1), derived from probability distributions for electron line density and power decay constant.

Weitzen in his work examined the relationship between range and three performance measures of meteor burst communication systems: average duty cycle, average throughput for a system which transmits fixed length message packets at a fixed data rate, and waiting time to deliver a fixed length message [58]. Duty cycle is determined as

$$\text{duty cycle} = \int\int\int_{\text{antenna pattern}} N_v(x,y,z)T_{ave}(x,y,z)dxdydz$$

where $N_v(x,y,z)$ is the number of bursts (per second per unit volume) that exceed the signal threshold, and $T_{ave}(x,y,z)$ is the average duration of a trail above the threshold at a point (x,y,z). Antenna pattern defines the meteor region for integration. Using Sugar's probabilistic model [50], Weitzen determined the average waiting time to transmit a fixed length message as

$$T_W = \frac{1}{N} \exp\left(\frac{T_m}{\tau}\right),$$

where N is the average number of trails per second with the required SNR, T_m is the message duration, and τ is the average burst duration. He showed that the optimum data rate R_{opt}, in terms of minimizing the waiting time T_W, agrees pretty well with the experimental data. For the 1260 km link and carrier frequency of 45 MHz, the calculated R_{opt} was 2 kbits/sec, and measured R_{opt} was about 3 kbits/sec.

A data base approach has been used to analyze data from the U.S. Air Force high-latitude meteor burst test bed [58]. Using expert system techniques for cost- and time-efficient search and classification of raw data, propagation and communication properties of a meteor burst channel can be represented as a function of operating frequency, time of a day, day and month of a year, and propagation mechanism. As an illustration of the technique, average throughput of the channel is plotted versus the time of day and transmission rate, for fully adaptive and fixed rate communication systems. Analysis of waiting times

to deliver a 1000-bit message, using a fixed rate system, shows that optimum data rates exist for every operating frequency.

2. METEOR TRAILS

The impact energy of a meteoric particle entering the earth's atmosphere produces heat which evaporates atoms from the meteor. Atoms move off at velocities equal to the velocity of the meteor, collide with the surrounding air and produce heat, light, and ionization in the form of a long, thin paraboloid. The resulting electron line density in the trail is proportional to the mass of a particle. During the trail formation, velocity of the meteor remains almost constant until it is completely evaporated.

No appreciable ionization is formed until the meteoric particles enter the relatively dense air at heights below 120 kilometers. The collision processes become more intense as the particles penetrate deeper into the atmosphere, and most meteors are completely evaporated before reaching the height of 80 kilometers above earth. This is the result of an approximately logarithmic manner in the decrease of the mean free path. The average distance that atoms can travel without colliding with air molecules is 5.4 meters at 120 kilometers of height, but it is only 3.8 millimeters at 80 kilometers [53]. High velocity particles produce

trails in the upper region of this 40 kilometer thick "meteor layer", and high mass particles are responsible for ionization at lower heights.

The length of a meteor trail can be defined as a distance between points on a trail that have threshold electron density. For sporadic meteors, the average length is 15 kilometers, but some trails can be as large as 50 kilometers. The resulting distribution of trail lengths appears to be independent of the threshold value, so the threshold can be chosen arbitrarily [15].

The initial radius of a meteor trail is significantly larger than the mean free path of atoms evaporating from the surface of a meteoric particle. The mean free path, itself, is directly proportional to air density [21] [18]. Being of a comet origin, meteors are best described as "dustballs", clusters of frozen gases covered with cosmic dust. Upon entering earth's atmosphere, dustballs are broken into fragments that evaporate separately, resulting in a trail larger than predicted only by looking at the initial mass. The mean initial radius at 80 kilometers of height is 0.65 meters, and it is 4.35 meters at 120

kilometers.

The electrons liberated by initial ionization disperse by a low rate diffusion, producing approximately Gaussian radial distribution of material. As the diffusion coefficient D varies from 1 m^2/sec at 85 kilometers of height to 140 m^2/sec at 115 kilometers [19], the trail will after one second have a radius from 2 to 20 meters, depending on its initial radius.

The presence of winds in the meteor region, ranging from 80 to 120 kilometers of height, affects dissipation and orientation of meteor trails. Those winds have typical velocities of 25 km/sec, and vertical gradients of up to 100 m/sec/km [34].

Most trails detected by radio means result from small particles whose practical lifetime, in communication terms, is a fraction of a second. Larger particles and resulting more densely ionized trails, with durations of a minute or an hour, are extremely rare.

2.1. Short-term Statistical Characteristics

2.1.1. Received Power

Energy reflected from a meteor trail is a function of several physical quantities: ionization density across and along the trail, radio wavelength, and the polarization of the incident wave relative to the trail. Orientation of the trail, its motion (as a part of the process of formation or due to atmospheric winds), and its straightness, are also significant.

It is convenient to divide the trails into two classes, underdense and overdense. Underdense trails are those with densities of up to 10^{14} electron lines per meter. It is low enough for the incident wave to pass through the trail, and the trail itself can be considered as an array of independent scatterers. Overdense trails have densities greater than 10^{14} electron lines per meter, what is high enough to prevent complete penetration of the incident wave, and to cause the reflection of waves in the same way that the ordinary ionospheric reflections occur.

Underdense trails are much more numerous, but their average duration at long wavelengths is less than a second. Overdense trails last from a couple of seconds to a minute or more. For both trail types, the effective duration is large compared to the formation time, and the trails may be considered to have a cylindrical shape.

The following models for underdense and overdense trails are, at best, useful approximations to the physical reality. They apply quite well to some of the trails observed, rather poorly to others, but a complete analysis involving all possible variables would be far too complex and would lead to results of a little practical use.

2.1.2. Power Received from Underdense Trails

Following the exponential decay model for underdense trails from Eshleman [14], Sugar derived the transmission equation for the case of point-to-point propagation as [50]

$$P_{su} = C_u \, q_1^2 \, \exp\left(-\frac{t}{b}\right). \qquad (2.1.2\text{-}1)$$

P_{ru} is the received power, q_1 is the underdense electron line density, b is the decay constant, and t represents the time measured from the trail formation. The proportionality constant C_u is of the form

$$C_u = \frac{G_T G_R \lambda^3 r_c^2 \sin^2\alpha P_T}{16\pi^2 R_T R_R (R_T + R_R)(1 - \cos^2\beta \sin^2\phi)} \cdot \exp\left(-\frac{8\pi^2 r_0^2}{\lambda^2 \sec^2\phi}\right), \qquad (2.1.2-2)$$

where

G_T and G_R are, respectively, the power gains of the transmitting and receiving antennas relative to an isotropic radiator in free space,

λ is the carrier wavelength in meters,

$r_c = 2.8 \times 10^{-15} m$ is the classical radius of the electron,

α is the angle between the electric vector at the meteor trail and R_R,

P_T is the transmitted power in watts,

R_T and R_R are, respectively, distances of transmitter and receiver from the point on the trail at which the reflection requirement is satisfied,

β is the angle between the trail and the plane of R_T and R_R,

ϕ is one half the included angle between R_T and R_R, and

r_0 is the initial radius of trail in meters.

Eq. (2.1.2-1) represents somewhat idealized viewpoint in deriving expressions for energy reflected from meteor trails, since some practical aspects have been ignored.

During the trail formation, but before a meteor reaches the first Fresnel zone, a weak reflection is obtained from the incomplete trail, coming primarily from the "head" of a trail. The reflected signal is shifted in frequency, due to relative motion of the effective reflecting point and the receiver antenna [9]. A maximum shift of the order of 5 kHz is possible for 50 MHz forward scatter, over a 1000 kilometer path. As the meteor approaches the first Fresnel zone for the trail, this frequency shift falls to zero. Not many trails have such orientation with respect to transmitter antenna as to produce this kind of specular reflection, and most of the time only weak Doppler shift is observed.

The effect of ionospheric winds is appreciable only for trails that last more than a second, a rare occasion for

underdense trails. A Doppler shift of received frequency can reach 18 Hz for 50 MHz carrier, and is associated with an average wind velocity of 25 m/sec. The wind shear can lead to formation of several local first Fresnel zones moving at different velocities, having Doppler shifts of 1 to 10 Hz, and the resulting composite signal fades in an irregular manner [33].

Polarization effects are represented by $\sin^2\alpha$ term in Eq. (2.1.2-2). For underdense trails and trail diameters much smaller than the wavelength, resonance may occur from restoring force that the electrons experience as the incident electric field displaces them from their equilibrium positions. This resonance may double the reflection coefficient and increase the received power by a factor of 4 [29].

2.1.3. Power Received from Overdense Trails

When the electron line density in a trail exceeds 10^{14} electrons per meter, the incident wave penetrates the trail until reaching a surface of sufficiently high electron density to be reflected. Thus, the model applied in

evaluating the reflected power from a trail is that of an expanding cylindrical reflector [50]. After a while, the electron line density everywhere inside the trail falls below critical value and underdense model again applies, but the radius of the trail is too large for the signal contribution to be significant.

The transmission equation is [25]

$$P_{so}(t) = C_o \sqrt{(k+t)\ \ln\left(\frac{aq_2}{k+t}\right)}, \quad t \le aq_2 - k \tag{2.1.3-1}$$

where the constants are defined as

$$C_o = 3.17 \cdot 10^{-3}\sqrt{D}\ \frac{P_T G_T G_R \lambda^2}{R_T^3},$$

$$k = \frac{0.1}{D}, \tag{2.1.3-2}$$

$$a = 7.14 \cdot 10^{-17}\ \frac{\lambda^2 \sec^2\phi}{D}.$$

The parameters involved are defined in Section 2.1.2.

2.1.4. Underdense Electron Line Density

Electron line density q_l of an underdense trail, representing the number of electrons per meter, is a random variable with probability density function [25]

$$f(q_l) = Q_l q_l^{-1.6}$$

$$= 0.6 \frac{q_{minu}^{0.6} q_{uu}^{0.6}}{q_{uu}^{0.6} - q_{minu}^{0.6}} q_l^{-1.6}, \quad q_{minu} \le q_l \le q_{uu} \qquad (2.1.4-1)$$

where $q_{uu} = 10^{14}$ e/m is the maximum electron line density for underdense trails. The corresponding cumulative distribution function of q_l is

$$F(q_l) = \frac{q_{uu}^{0.6}}{q_l^{0.6}} \frac{q_l^{0.6} - q_{minu}^{0.6}}{q_{uu}^{0.6} - q_{minu}^{0.6}}, \quad q_{minu} \le q_l \le q_{uu}. \qquad (2.1.4-2)$$

The minimum observable electron line density q_{minu} is a function of communication system parameters: power spectral density N_0 of Gaussian galactic noise, data rate R and $P_{b\,max}$, the maximum allowable bit error rate in transmission. It is also dependent on the chosen modulation scheme, and

for BPSK modulation has the form

$$q_{minu} = \sqrt{\frac{N_0 R}{C_u}}\ \mathrm{erfc}^{-1}(2P_{bmax}), \qquad (2.1.4-3)$$

where $erfc^{-1}(\cdot)$ denotes the inverse of a complementary error function.

2.1.5. Overdense Electron Line Density

The electron line density q_2 of an overdense trail, representing the number of electrons per meter, is a random variable with probability density function [25]

$$f(q_2) = Q_2\ q_2^{-1.5}$$
$$= \frac{1}{2}\ \frac{q_{mino}^{0.5}\ q_{uo}^{0.5}}{q_{uo}^{0.5} - q_{mino}^{0.5}}\ q_2^{-1.5}, \quad q_{mino} \le q_2 \le q_{uo}, \qquad (2.1.5-1)$$

where $q_{uo} = 10^{16}$ e/m is the maximum electron line density for overdense trails. The corresponding cumulative distribution function of q_2 is

$$F(q_2) = \frac{q_{uo}^{0.5}}{q_2^{0.5}} \frac{q_2^{0.5} - q_{mino}^{0.5}}{q_{uo}^{0.5} - q_{mino}^{0.5}}, \quad q_{mino} \le q_2 \le q_{uo}. \qquad (2.1.5-2)$$

The minimum electron line density of overdense trails is equal to the larger of the constants q_T and q_{uu},

$$q_{mino} = \max\ (q_T, q_{uu}),$$

with q_T given by

$$q_T = \frac{e}{a} \left(\frac{C_u}{C_o}\right)^2 q_{minu}^4.$$

2.1.6. Underdense Power Decay Constant

The decay constant b is a random variable with Rayleigh probability density function [25],

$$f(b) = \frac{b}{\alpha^2} \exp\left(-\frac{b^2}{2\alpha^2}\right), \quad 0 \le b < \infty, \qquad (2.1.6-1)$$

where the Rayleigh parameter α is

$$\alpha = \sqrt{\frac{2}{\pi}}\, E\{b\} = \sqrt{\frac{2}{\pi}}\, \bar{b}.$$

The corresponding cumulative distribution function of b is

$$F(b) = 1 - \exp\left(-\frac{b^2}{2\alpha^2}\right), \quad 0 \le b < \infty. \tag{2.1.6-2}$$

If the signal duration is defined as the time required for the signal amplitude to fall to $1/e$ of its initial value, the average value of the decay constant b is [50]

$$\bar{b} = \frac{\lambda^2 \sec^2 \phi}{16\pi^2 D}, \tag{2.1.6-3}$$

with D being the diffusion coefficient in square meters per second, a function of height [8].

2.1.7. Underdense Burst Duration

Duration of an underdense trail, measured from the instant of a trail formation to the point when electron line density q_l falls to the threshold value q_{minu}, can be expressed as

$$t_{BU} = b \cdot \ln\left(\frac{q_l}{q_{minu}}\right)^2. \qquad (2.1.7-1)$$

This is a function of two random variables, q_l and b, and by transforming their probability density functions we obtain

$$f(t_{BU}) = \frac{0.8}{1-x} \int_b^{\infty} \frac{1}{b} \exp\left(0.8\frac{t_{BU}}{b}\right) f(b)db, \qquad (2.1.7-2)$$

the probability density function for t_{BU}. The expected value of underdense burst duration is then

$$\bar{t}_{BU} = 3.33\ \bar{b}\ \frac{1 - x + x\ln x}{1 - x}, \qquad (2.1.7-3)$$

where the average decay constant $\bar{b}$ is defined by Eq. (2.1.6-3). The parameter x from Eqs. (2.1.7-2) and (2.1.7-3) is equal to

$$x = \left(\frac{q_{minu}}{q_{uu}} \right)^{0.6} .$$

2.1.8. Overdense Burst Duration

The power received from an overdense trail is a function of time, and has a parabolic shape. The duration of an overdense burst is defined as the time distance between points with the same power threshold value, and is approximately equal to [25]

$$t_{BO} = 0.95 a q_2 \sqrt{1 - \frac{q_T}{q_2}}, \qquad q_{mino} \leq q_2 \leq q_{uo}.$$

The average overdense burst duration is then

$$\bar{t}_{BO} = 1.9\alpha Q_2\sqrt{q_T}\ \left(\sqrt{\frac{q_{uo}}{q_T}-1} - \sqrt{\frac{q_{mino}}{q_T}-1} + \right.$$

$$\left. + \cos^{-1}\sqrt{\frac{q_T}{q_{mino}}} - \cos^{-1}\sqrt{\frac{q_T}{q_{uo}}}\right). \qquad (2.1.8-1)$$

2.1.9. Trail arrivals

Experimental evidence shows that the arrival of meteor trails with suitable orientation for communication can be modeled as a Poisson random process [41]. Thus, the probability of having exactly k trails in an observation time T_D is

$$P\{\text{k trails in } T_D\} = \frac{1}{\text{k!}}\left(\frac{T_D}{t_I}\right)^k \exp\left(-\frac{T_D}{t_I}\right), \qquad (2.1.9-1)$$

where t_I is the mean time between trail appearances.

To determine the mean time between meteor trail arrivals, more complex models than the reference method from [41] are needed, but they require extensive use of computational resources. The models may include the effects of "hot spots" and nulls in the spatial arrival pattern,

that are due to geometrical constraints [20] [26] [13].The other way is to perform multidimensional integrations over the antenna patterns for the specific link, taking into consideration the nonuniform spatial distribution of meteor trails [56] [8] [57] [45]. The spatial distribution of meteor trail arrivals is derived from astronomical data gathered for meteor orbits [50].

The mean time between underdense trails, whose electron line density q_1 is in an interval (q_a, q_b), is then [25] [55]

$$t_{1U} = \frac{1}{19.1667 \cdot \phi \sin\phi \ (R_R \zeta)^2} \frac{q_a q_b}{q_b - q_a}, \qquad (2.1.9-2)$$

where ζ is the idealized antenna beamwidth. The same formula is valid for the overdense trails, except for the scaling constant,

$$t_{1O} = \frac{1}{3 \cdot \phi \sin\phi \ (R_R \zeta)^2} \frac{q_a q_b}{q_b - q_a}, \qquad (2.1.9-3)$$

in this case when q_2 is in (q_a, q_b). These are empirical relationships, and to obtain meaningful results we must

have that, e.g., $q_1 > 10^{13}$ electrons per meter for a 1000 kilometer link and $\zeta = 46°$. The quantity q_2 is limited to the maximum possible electron line density of meteor trails.

2.1.10. Power Spectral Density of the Received Noise

In the frequency spectrum of interest to meteor burst communication, the wideband noise is either of galactic origin, picked by receiver antenna, or due to thermal agitations in the receiver itself. Its one-sided power spectral density is of the form [25]

$$N_0 = kT_0\left[\frac{104}{L_R}\left(\frac{\lambda}{15}\right)^{2.3} + F\right] \qquad (2.1.10-1)$$

where $k = 1.38 \times 10^{-23} J/K$ is the Boltzmann's constant, $T_0 = 290°K$ is the room temperature, L_R is the power loss between the antenna and the receiver, F is the receiver noise figure, and λ is the carrier wavelength in meters. Values used in this work, for calculations and simulations, are $L_R = 1.3$ and $F = 2.5$.

2.2. Long-Term Statistical Characteristics

The statistical characteristics of a meteor-burst channel change during day and night, and depend on the season of the year. Statistical variations are also associated with the characteristics of a communication system, and geographical locations of transmitters and receivers.

2.2.1. Diurnal Variations

Variations in meteor propagation on a daily basis are due to astronomical factors: meteor arrival rate, meteor velocities, and locations of effective radiants, points in the sky where meteors appear to come from.

Meteor arrival rate varies sinusoidally during 24-hour period, with the maximum around 6 a.m. and minimum around 6 p.m., the ratio of maximum to minimum being close to 4 [21].

The average meteor velocity has similar sinusoidal variation as the meteor arrival rate, and extrema located at the same hours of the day. A variation of 10 to 15 km/sec above and below a daily mean velocity of 35 to 45 km/sec

appears to be typical [32]. The velocity variations lead to a variation in the height of a trail. Since the diffusion coefficient is a function of height, average burst durations will vary over a 2 to 1 range through the day.

Because of the orbital motion of the earth, most meteors appear to have radiants in the hemisphere ahead of the earth. As the earth rotates, the position of the predominant radiants changes relative to the transmission path, and the location of the "hot spot" moves around. The values of the geometric factors in transmission equation will consequently vary, and a change in received power will occur. The effects of radiant changes are relative to transmission path orientation, be it north-south or east-west [27].

2.2.2. Seasonal Variations

Variations in meteor-burst propagation characteristics are primarily the consequence of meteor characteristics, and there is little evidence on ionospheric influence, with the possible exception of D-region absorption.

The peak of meteoric activity occurs during the summer months of June, July, and August. It is then diminishing steadily through autumn and winter, reaching its minimum in February, only to rise again with the coming of spring.

The question of year to year variations is still unresolved, although some changes have been observed.

2.2.3. Geographic and Parametric Variations

Location and orientation of the transmission path, operating frequency, antenna patterns, and path length are the main factors that affect statistical characteristics of a meteor burst channel.

Propagation characteristics are somewhat influenced by continuous-mode D-region ionospheric scattering, and a number of weaker meteor signals are masked out, contributing to a change in observed occurrence of underdense and overdense trails. At frequencies higher than 30 MHz, the influence of ionospheric scatter is minimal, what determines the minimum usable frequency of a meteor burst communication systems.

The normal attenuation of signals due to D-region absorption is slightly higher for meteor signals, since the D-region is below meteor region and signals encounter longer paths within the absorbing region. This absorption can increase significantly at times of ionospheric disturbance, but its sporadic nature does not influence average characteristics of the meteor burst propagation [31].

Diurnal variations in meteor arrival rate and percentage of useful communication time (duty cycle) are strongly dependent on antenna patterns. A great increase in duty cycle is observed when receiver antennas are directed to the north of the great circle path during the morning hours, or to the south in evening hours [44].

3. METEOR BURST COMMUNICATION SYSTEM

Digital data are transmitted over a meteor burst channel using binary phase-shift keying modulation (BPSK), at a constant data rate R. The transmitted signal is

$$s(t) = \pm\sqrt{2P_T}\cos\omega_0 t, \quad 0 \le t \le T_b,$$

where P_T is the transmitter power, $f_0 = \omega_0/2\pi$ is a carrier frequency, and $T_b = 1/R$ is the bit duration.

Multipath phenomena are encountered in meteor burst communications only at high data rates. Overdense trails are then the dominant propagation medium, since there appear very few underdense trails with electron line densities high enough to provide sufficient scattered signal power. At low data rates underdense trails are much more numerous, they act as small coherent sources and scattered continuous-wave signals exhibit good space and frequency correlation. In those circumstances the phase of the received signal is assumed constant, representing only the

gross time delay due to the average distance which a signal must propagate. Such delay amounts only to a shift in time origin.

The signal received from an underdense or overdense trail is of the form

$$r(t) = \pm A\cos\omega_0 t + n(t)$$
$$= \pm\sqrt{2P_s}\cos\omega_0 t + n(t), \quad 0 \le t \le T_b,$$

where $A = \sqrt{2P_s}$ is the random amplitude of a signal scattered from a meteor trail, P_s is the received signal power, and $n(t)$ is a Gaussian noise with one-sided power spectral density defined in Eq. (2.1.10-1). BPSK signals have the same energy $E_b = P_s T_b$, and the optimum decision threshold in a correlation receiver is set to $V_t = 0$ volts. Since the attenuation of the signal is always positive, the optimum decision regions are invariant to radial scaling of received signals. Under these conditions, a correlation or matched-filter receiver structure is still optimum, completely independent of the fact whether amplitude A or probability density function of amplitudes $f(A)$ is known precisely [60].

For underdense trails, the received power P_s is equal to $P_{s,u}$ from Eq. (2.1.2-1), and amplitude A becomes a function of two random variables, electron line density q_l and decay constant b. Transforming their density functions from Eqs. (2.1.4-1) and (2.1.6-1), we obtain the probability density of underdense signal amplitudes A_u as

$$f(A_u) = 2.46 Q_l A_u^{-1.6} \int_{y_1}^{y_2} \exp\left(-\frac{0.2t}{\alpha y} - y^2\right) y\, dy, \qquad (3-1)$$

valid in the interval

$$\sqrt{2C_u}\, q_{minu} \le A_u \le \sqrt{2C_u}\, q_{mino}.$$

The integration limits in Eq. (3-1) are

$$y_1 = \frac{t}{2\alpha\sqrt{2}\,\ln\left(\frac{q_{minu}}{A_u}\sqrt{2C_u}\right)},$$

$$y_2 = \frac{t}{2\alpha\sqrt{2}\,\ln\left(\frac{q_{mino}}{A_u}\sqrt{2C_u}\right)}.$$

For overdense trails, the received power P_s is equal to P_{so} from Eq. (2.1.3-1), and amplitude A is consequently a function of one random variable, electron line density q_2. Transforming its distribution from Eq. (2.1.5-1), probability density for overdense signal amplitudes A_o becomes

$$f(A_o) = \frac{Q_2 A_o^3 \sqrt{a}}{C_o^{3/4}(k+t)^{3/2}} \exp\left[-\frac{A_o^4}{8C_o^2(k+t)}\right]$$

valid in the interval

$$\sqrt{2C_o}\left[k \ln\left(\frac{a q_{mino}}{k}\right)\right]^{1/4} \leq A_o \leq \frac{a q_{uo}}{e}\sqrt{2C_o}.$$

Probability density functions of both underdense and overdense received signal amplitudes are too complicated as to gain some useful insight into the detection process.

3.1. Uncoded Transmission

3.1.1. Transmission over Underdense Trails

The conditional bit error probability assuming particular values of q_1 and b for a given burst, can be expressed in terms of the received power P_{su} from Eq. (2.1.2-1) as

$$P_{bu}(q_1, b; t) = P\{\epsilon \mid q_1, b; t\}$$
$$= \frac{1}{2} \, erfc \sqrt{\frac{C_u q_1^2}{N_0 R} \exp\left(-\frac{t}{b}\right)},$$

when BPSK modulation is used, and a packet is positioned at the beginning of a burst. The receiver bandwidth is equal to the bit rate R, i.e. their ratio is 1 bit/sec/Hz. Bit error rate is a continuous function of time t, but we will instead observe the received power P_{su} within the burst in discrete time instants $t_i = i/R$, that correspond to bit intervals. The conditional probability that the i-th bit in a packet is in error is then

$$P_{bu}\left(q_1, b; \frac{i}{R}\right) = P\left\{\epsilon \mid q_1, b; \frac{i}{R}\right\}$$
$$= \frac{1}{2} \, erfc \sqrt{\frac{C_u q_1^2}{N_0 R} \exp\left(-\frac{i}{Rb}\right)}. \qquad (3.1.1-1)$$

To simplify the analysis, we assumed that P_{su} remains constant during the bit interval and equal to the power at the end of the interval. This is a 'worst case' approach on a small scale, since the actual signal-to-noise ratio for every bit will be better than the one used in calculations.

The conditional probability that the packet N-bits long is correct is accordingly

$$P_{cu}(q_1, b) = P\{C \mid q_1, b\}$$
$$= \prod_{i=1}^{N} \left[1 - P_{bu}\left(q_1, b; \frac{i}{R}\right)\right]. \qquad (3.1.1-2)$$

Using the continuous version of the total probability theorem, we obtain the probability of correct packet reception in the integral form

$$P_{cu} = P\{C\}$$
$$= \int_{b=0}^{\infty} \int_{q_1=q_{minu}}^{q_{uu}} P_{cu}(q_1, b) f(b) f(q_1) dq_1 db. \qquad (3.1.1-3)$$

When more than one data packet is sent during the burst, the respective packet beginnings will be separated by the packet length $T_p = N/R$. Following the reasoning for Eq. (3.1.1-1), the conditional bit error probability for the packet in the k-th time slot will be

$$P_{bu}\left(q_1, b; \frac{i}{R} + kT_p\right) = P\left\{\epsilon \mid q_1, b; \frac{i}{R} + kT_p\right\}$$

$$= \frac{1}{2}\, erfc\sqrt{\frac{C_u q_1^2}{N_0 R}\, \exp\left[-\frac{1}{b}\left(\frac{i}{R} + kT_p\right)\right]}. \qquad (3.1.1-4)$$

The conditional probability that N-bits long packet sent during the k-th time slot is received correctly is then

$$P_{cu}(q_1, b; kT_p) = P\{C \mid q_1, b; kT_p\}$$

$$= \prod_{i=1}^{N}\left[1 - P_{bu}\left(q_1, b; \frac{i}{R} + kT_p\right)\right], \qquad (3.1.1-5)$$

and the total probability is calculated using the same double integration as in Eq. (3.1.1-3)

$$P_{cu}(kT_p) = P\{C\}$$

$$= \int_{b=0}^{\infty} \int_{q_1=q_{min}}^{q_{max}} P_{cu}(q_1, b; kT_p) f(b) f(q_1) dq_1 db. \qquad (3.1.1-6)$$

3.1.2. Transmission over Overdense Trails

The conditional bit error probability assuming a particular value of electron line density q_2, can be expressed in terms of received power P_{so} from Eq. (2.1.3-1) as a continuous function of time

$$P_{bo}(q_2; t) = P\{\epsilon \mid q_2; t\}$$

$$= \frac{1}{2} \, erfc \left(\frac{C_o}{N_0 R} \sqrt{(k+t) \, \ln\left(\frac{\alpha q_2}{k+t}\right)} \right)^{\frac{1}{2}},$$

for BPSK modulation, receiver bandwidth equal to data rate, and a data packet positioned at the beginning of a burst. When the received power is observed in discrete time instants $t_i = i/R$, at the end of a bit interval, the conditional probability that the i-th bit in a packet is in error is

$$P_{bo}\left(q_2;\frac{i}{R}\right) = P\left\{\epsilon \mid q_2;\frac{i}{R}\right\}$$

$$= \frac{1}{2}\, erfc\left(\frac{C_o}{N_0 R}\sqrt{\left(k+\frac{i}{R}\right)\ln\left(\frac{aq_2}{k+i/R}\right)}\right)^{\frac{1}{2}}, \quad (3.1.2-1)$$

assuming that P_{so} remains constant during the bit interval and is equal to the power received at the end of the interval.

Under these conditions, the corresponding conditional probability of a packet N-bits long being correct becomes

$$P_{co}(q_2) = P\{C \mid q_2\}$$

$$= \prod_{i=1}^{N}\left[1 - P_{bo}\left(q_2;\frac{i}{R}\right)\right]. \quad (3.1.2-2)$$

The total probability of correct packet reception is then evaluated as

$$P_{co} = P\{C\}$$

$$= \int_{q_2=q_{min}}^{q_{uo}} P_{co}(q_2) f(q_2) dq_2. \quad (3.1.2-3)$$

For packets not positioned at the beginning of a burst, the calculation of a bit error rate and the corresponding probability of correct packet reception is similar to the one performed in Eqs. (3.1.1-4) and (3.1.1-5).

3.2. Coded Transmission

For coded transmission, convolutional codes were chosen because of their superior performance compared to block codes, for the same implementation complexity of the encoder-decoder [49].

We did not consider the class of burst-error correcting codes since very few statistical data are available on the existence or length of meteor burst channel memory. Although exponential decay of received power toward the end of a burst in underdense case leads to conclusion that bit errors become more frequent, the noise model from Eq. (2.1.10-1) indicates that for narrowband modulation the noise may be considered white, and noise samples in successive bit intervals are consequently independent.

For higher data rates, or for spread spectrum systems, noise can not be taken as white any more, since its power spectral density will change inside the signaling bandwidth. Noise samples become dependent, and this noise model predicts the appearance of channel memory. If experimental data confirm these conclusions, use of interleaving will become necessary to 'randomize' transmission errors and maintain the performance of convolutional codes, which are not best suited for burst errors. Recent experimental data in fact indicate that the addition of a low-degree interleaver provides substantial improvement [11]. The results are not directly applicable to our work since BCH codes were used for forward error correction, and the only conclusion that can be drawn is that the burst length is relatively short (about 5 bits at data rate of 4800 bits/sec.)

We considered both rate-1/n and rate-k/n convolutional codes. Rate-1/n codes provide for superior error-correcting performance, at the cost of substantial lengthening of the original packet. For this reason, rate-1/n codes with $n > 2$ are at disadvantage in meteor burst communications, since the coded packet length becomes

prohibitively large and will often exceed burst duration, resulting in the loss of many bits as their time slots fall beyond the receiver threshold point. Rate-k/n codes are less powerful but more compact, and their error-correcting capability is not easily overwhelmed by the strong limiting factor of relatively short burst durations, particularly when k/n ratio approaches to 1. In our work, code rates of 1/2, 3/4, and 7/8 were considered.

When decoding convolutional codes, the error-correcting capability is difficult to state precisely. With maximum likelihood decoding a code can correct t errors within 3 to 5 constraint lengths, and it is defined in terms of the free distance of a code d_f [1]

$$t = \left\lfloor \frac{d_f - 1}{2} \right\rfloor.$$

The exact length depends on actual error distribution, and for a particular code and error pattern, transfer functions methods are used to obtain bounds [49]. In our case the

---

1 The notation $\lfloor x \rfloor$ signifies the greatest integer smaller than or equal to x.

problem is further aggravated by the fact that signal-to-noise ratio is not constant within the packet time duration T_p, but rather changes as the received power varies with time.

A way to overcome these difficulties was to use the notion of cutoff rate R_0 for binary transmission

$$R_0 = 1 - \log_2(1+D) \quad \text{bits/symbol} ,$$

in order to decouple the influence of the coding channel characterized by R_0 from the coding technique [47]. For example, in case of a rate-1/2 code with constraint length $K = 7$ and hard decision decoding, the decoded bit error rate is upper bounded by [47]

$$P_{\text{b coded}} \leq 18D^{10} + 105.5D^{12} + 702D^{14} + 5816.5D^{16} + \ldots , \quad (3.2-1)$$

where the parameter D is

$$D = 2\sqrt{P_b(1-P_b)} , \quad (3.2-2)$$

and P_b represents the channel bit error rate. $P_{b\,coded}$ and P_b are conditional probabilities assuming either q_1 and b in underdense case, or q_2 when overdense bursts are involved.

For the rate-k/n codes, we used the following upper bound on decoded bit error probability [35]

$$P_{b\,coded} \leq \frac{1}{k} \sum_{j=d_f}^{\infty} w_j \, \frac{1}{2} erfc \sqrt{\frac{jE_s}{N_0}}, \qquad (3.2-3)$$

where d_f is the free distance of a code, $E_s = E_b r$ is the symbol energy, $r = k/n$ is the code rate, E_b is the bit energy, and N_0 is the noise power spectral density. Code-specific coefficients w_j, for different values of the code constraint length, are summarized in tables [10]. This is also a conditional probability, as explained above.

Infinite-level quantization results in 2.2 dB improvement over two-level or hard quantization. It can be approximated by the 3-bit soft decisions about the channel output, resulting in a 2 dB gain over the hard quantized binary symmetric channel.

Bounds on decoded bit error rate are derived for constant signal-to-noise ratio and arbitrarily large path memory, i.e. the depth of the input bit history stored by the decoder and used in a decision about the value of a particular bit. Nevertheless, it was shown in [23] that a fixed amount of path history, namely 4 or 5 times the constraint length, is sufficient to limit the degradation from the optimum decoder performance to about 0.1 dB for binary-symmetric and Gaussian channels. In a meteor burst channel the signal-to-noise ratio is constantly changing, but most of the time it does not change substantially during the fixed decoding delay, and we took it to be constant for the bits along one path memory length. Furthermore, the decision about a specific bit is brought by analyzing the trellis branches consisting of bits that all have equal or higher signal-to-noise ratios than the bit in question.

3.2.1. Transmission over Underdense Trails

Parameter D from Eq. (3.2-2) in this case takes the form

$$D = 2\sqrt{P_{bu}\left(q_1, b; \frac{i}{R}\right)\left[1 - P_{bu}\left(q_1, b; \frac{i}{R}\right)\right]},$$

where the conditional bit error probability $P_{bu}(q_1, b; i/R)$ is given by Eq. (3.1.1-1). After calculating the values for $P_{\text{bu coded}}$ according to Eqs. (3.2-1) or (3.2-3), the conditional probability that encoded packet will be correctly received is found as the product

$$P_{\text{cu coded}}(q_1, b) = P\{C \mid q_1, b\}$$
$$= \prod_{i=1}^{N} \left[1 - P_{\text{bu coded}}\left(q_1, b; \frac{i}{R}\right)\right],$$

assuming particular values for electron line density and decay constant in a given underdense burst. It then follows that

$$P_{\text{cu coded}} = P\{C\}$$
$$= \int_{b=0}^{\infty} \int_{q_1=q_{minu}}^{q_{uu}} P_{\text{cu coded}}(q_1, b) f(b) f(q_1) dq_1 db. \qquad (3.2.1-1)$$

represents the total probability of receiving an error-free packet.

3.2.2. Transmission over Overdense Trails

Following the same steps as in Sec. 3.2.1., we obtain the parameter D in the form

$$D = 2\sqrt{P_{bo}\left(q_2;\frac{i}{R}\right)\left[1-P_{bo}\left(q_2;\frac{i}{R}\right)\right]},$$

with $P_{bo}(q_2;i/R)$ from Eq. (3.1.2-1). The conditional probability that a coded packet is correctly received is

$$P_{\text{co coded}}(q_2) = P\{C \mid q_2\} = \prod_{i=1}^{N}\left[1-P_{\text{bo coded}}\left(q_2;\frac{i}{R}\right)\right],$$

assuming a particular value for electron line density. Finally, the corresponding total probability

$$P_{\text{co coded}} = P\{C\} = \int_{q_2=q_{mino}}^{q_{uo}} P_{\text{co coded}}(q_2)f(q_2)dq_2. \qquad (3.2.2-1)$$

is the probability of receiving the coded data packet correctly.

4. COMMUNICATION SYSTEM PERFORMANCE MEASURES

Performance measures used in this work to characterize a meteor burst communication system and transmission protocols are: Throughput rate, waiting time to receive a message correctly, and probability of receiving the correct message within a specified observation time. They are functions of communication system parameters, but primarily dependent on the chosen communication protocol. An additional performance measure, duty cycle, is also evaluated, and it is a function of system parameters only.

We will examine two automatic-repeat-request (ARQ) protocols for point-to-point data transmission over a meteor burst channel. We will refer to them as "stop-and-wait" and "selective-repeat" strategies, since they are similar to those described in [51]. The main difference is in the channel behavior, since the meteor burst channel is not continuous but rather intermittent. The time of its appearance and its duration are random variables, what is described in detail in Chapter 2. In both protocols we differentiate between a "forward" and a "feedback" channel, the former being used for sending information messages from

transmitting to the receiving end of a link, and the latter for transmission of acknowledgement information from receiver to the transmitter.

The third existing ARQ protocol, "go-back N", where the transmitter goes back to the rejected message and continues sending data blocks from there, is not considered. Large amount of available memory for data storage in today's computer-to-computer communications alleviates past problems with sorting data packets not received in the right order and, instead of "go-back N", more efficient "selective-repeat" scheme can be used.

In a "stop-and-wait" strategy only one message is sent during the available burst time, as soon as the probe signal indicates the opening of a channel. (In this work, the message is comprised of a single data packet.) Although in some systems the pilot signal is a back-scattered probe signal continuously sent by the transmitting terminal itself, we took it here to be a forward-scattered signal originated at the receiving end of a point-to-point data communications link. After completing the message, the transmitting terminal has to wait for the receiver response

not because of the processing in the receiver, since it is done in the idle time between trails. The main cause of the delay is the fact that a receiver must wait for the next available trail to send back its acknowledgment, after checking the validity of a received packet.

Data packet is N-bits long, consisting of k information bits and r bits for error detection and/or correction. Upon examining the parity of the incoming packet, or performing the cyclic redundancy check (CRC), the receiver sends back an s-bit long positive (ACK) or negative (NAK) acknowledgment signal during the next available burst. The transmitter repeats the current packet if it received the NAK signal or proceeds to a new packet of data in case of the ACK signal. The repeated or the new packet are sent immediately upon reception of the ACK/NAK signal, within the same burst.

In a hybrid FEC-ARQ scheme, forward error correction is used in addition to ARQ. Before sending back the acknowledgement message, the receiver tries to correct transmission errors in the incoming packet, if any are discovered in the parity check or CRC procedure.

In a "selective-repeat" strategy, the transmitter sends as many messages (data packets) as the duration of a current burst allows. It determines the burst duration with the help of a probe signal from the receiver. Message transmission starts with the indication of a channel opening, and stops when the loss of a probe signal shows that a channel is terminated. The communication is full-duplex during the burst duration, and ceases in the idle time between bursts. Forward channel is used for the transmission of new and repeated packets. Along the feedback channel goes the information about correctly received packets, and the numbers of packets that have to be repeated. If no acknowledgment is received for a particular packet, it is regarded as a request for retransmission. Receiver probe signal is used as the carrier for acknowledgment signals. Data packets have the same structure as in a stop-and-wait strategy.

4.1. Throughput Rate

4.1.1. Stop-and-Wait Strategy

The throughput rate T_{SW} in a stop-and-wait strategy is defined as the ratio of the number of information bits per packet to the total average number of bits that had to be transmitted before a particular packet is received correctly [5], that is

$$T_{SW} = \frac{N - r}{(N + \tau + s)E} \quad . \qquad (4.1.1-1)$$

N is the total number of bits in a packet, r is the number of parity bits, and s is the bit length of acknowledgement signals. τ denotes the average number of idle bit times counted from the last bit of a data packet transmitted and the first bit of an ACK/NAK message received. The acknowledgement message is positioned at the beginning of the next available burst, as illustrated in Fig. 2. E represents the average number of transmissions of one packet accumulated to the moment the transmitter proceeds to a new packet of data.

The probability Δ that a given transmission of a packet at the same time happens to be the last one is

$$\Delta = P_c + P_e \ , \qquad (4.1.1-2)$$

where P_c is the probability that a packet is received correctly. P_e is the probability that a received packet contains an undetectable error pattern, and is erroneously considered to be correct by the receiver.

The underlying assumption for Eq. (4.1.1-2) is that ACK/NAK signal is always received correctly with probability equal to 1. In practice, this can be closely achieved by heavy coding of acknowledgment signals. These signals are short and even with very low code rates they will occupy a small amount of a burst time. Furthermore, they are sent at the beginning of a burst when bit error probability is at its minimum. Since the burst time is valuable, the probe signal itself carries the acknowledgment information.

For an average linear (n,k) code, the undetected error probability P_e is bounded by [30]

$$P_e \leq 2^{-(n-k)}(1-P_c).$$

For a double-error-correcting primitive BCH code it is bounded by

$$P_e \leq 2^{-(n-k)}.$$

It means that for either of these codes, that are often used in error detection, P_e may be neglected in comparison to P_c for any practical packet length. The same conclusion is valid for the case when cyclic redundancy check (CRC) polynomials are used for detecting the errors in a received packet. Thus, we continue our derivation with Eq. (4.1.1-2) reduced to

$$\Delta = P_c. \qquad (4.1.1-3)$$

Now, the probability that we need exactly $n = i$ transmissions of a packet to receive it correctly, expressed in terms of probability Δ, is

$$P\{n = i\} = \Delta_i \prod_{k=0}^{i-1} (1 - \Delta_k),$$

meaning that before the i-th successful transmission there had been $(i-1)$ unsuccessful attempts. By definition, we have that $\Delta_0 = 0$. Substituting the value for Δ from Eq. (4.1.1-3), we have

$$P\{n=i\} = P_{ci} \prod_{k=0}^{i-1} (1 - P_{ck}), \qquad (4.1.1-4)$$

where P_{ci} and P_{ck} are the total probabilities of correct packet reception during the i-th and k-th transmission, respectively. In addition, for $k=0$ we define that $P_{c0} = 0$. The indexing of P_c is still necessary, since we are talking about transmissions over successive bursts which, in general, have different physical properties.

The total probability that a packet is received correctly during a particular try can be expressed as

$$P_c = P_u \int_{q_1} \int_{b} P\{C \mid q_1, b\} f(q_1) f(b)\, db\, dq_1 + \\ + P_o \int_{q_2} P\{C \mid q_2\} f(q_2)\, dq_2,$$

where the integration goes over all possible values for underdense and overdense electron line densities q_1 and q_2, and underdense decay constant b. Following the derivation from Eqs. (3.1.1-2) and (3.1.1-3) for the underdense case, and from Eqs. (3.1.2-2) and (3.1.2-3) for the overdense, the total probability can be expressed in the following form

$$P_c = P_u P_{cu} + P_o P_{co}. \qquad (4.1.1-5)$$

The probability of an underdense trail appearance P_u is the ratio of the expected number of underdense trails to the total expected number of trails (underdense and overdense), during some observation time T_D. It is equal to

$$P_u = \frac{T_D/t_{IU}}{T_D/t_{IU} + T_D/t_{IO}}$$

$$= \frac{t_I}{t_{IU}}, \qquad (4.1.1-6)$$

where t_{IU} and t_{IO} are the mean times between underdense and overdense trails, respectively, as defined in Eqs.

(2.1.9-2) and (2.1.9-3). Statistical parameter t_I is the mean time between arrivals for the combined process consisting of all the trails, regardless of type, and is defined in Eq. (4.2-3). Similarly, the probability of an overdense trail appearance P_o is the ratio of the expected number of overdense trails to the total expected number of trails

$$P_o = \frac{T_D/t_{IO}}{T_D/t_{IU} + T_D/t_{IO}}$$

$$= \frac{t_I}{t_{IO}}. \qquad (4.1.1-7)$$

Using the expression from Eq. (4.1.1-4), the average number of transmissions is

$$E = \sum_{i=1}^{\infty} iP\{n = i\}$$

$$= \sum_{i=1}^{\infty} iP_{ci} \prod_{k=0}^{i-1} (1 - P_{ck}). \qquad (4.1.1-8)$$

The way P_{cu} and P_{co} are calculated in Eqs. (3.1.1-3) and (3.1.2-3) is equivalent to averaging over the ensemble of underdense and overdense trails, respectively. As a result,

total probabilities P_c from Eq. (4.1.1-5) for any particular transmission attempt are statistically independent of each other, and will have identical values. Thus, Eq. (4.1.1-8) is simplified to

$$E = \sum_{i=1}^{\infty} iP_c(1-P_c)^{i-1}. \qquad (4.1.1-9)$$

Performing the summation of a geometric series in Eq. (4.1.1-9), the average number of packet transmissions becomes

$$E = \frac{1}{P_c}. \qquad (4.1.1-10)$$

Substituting this result into the Eq. (4.1.1-1), the throughput rate follows as

$$T_{sw} = \frac{N-r}{N+\tau+s} P_c. \qquad (4.1.1-11)$$

Dividing both the numerator and denominator in Eq. (4.1.1-11) with the bit rate R, we obtain

$$T_{SW} = \frac{T_p - T_r}{T_p + T_{idle} + T_s} P_c, \qquad (4.1.1-12)$$

where T_p, T_s, and T_r are the durations of a data packet, ACK/NAK signal, and parity bits, respectively. T_{idle} is the average idle communication time, measured from the end of a data packet transmitted to the beginning of an acknowledgement signal coming over the next available trail.

Idle communication time t_{idle} is a random variable, whose value is

$$t_{idle} = x - T_p,$$

with x representing the time difference between two consecutive trail appearances or, in fact, the distance between two successive Poisson points of a combined process. With respect to the probability density function for x [42]

$$f(x) = \frac{1}{t_l} \exp\left(-\frac{x}{t_l}\right),$$

we find the average value for t_{idle} as

$$\bar{t}_{idle} = T_{idle} = \int_0^{\infty} (x - T_p) f(x) dx$$
$$= t_l - T_p. \qquad (4.1.1-13)$$

Combining Eqs. (4.1.1-5) through (4.1.1-7), and (4.1.1-12) and (4.1.1-13), the final expression for the throughput rate becomes

$$T_{SW} = \frac{T_p - T_r}{t_l + T_s} \left(\frac{t_l}{t_{lU}} P_{cu} + \frac{t_l}{t_{lO}} P_{co} \right), \qquad (4.1.1-14)$$

when stop-and-wait strategy is used. It is, in fact, the sum

$$T_{SW} = \frac{T_p - T_r}{t_l + T_s} \frac{t_l}{t_{lU}} P_{cu} + \frac{T_p - T_r}{t_l + T_s} \frac{t_l}{t_{lO}} P_{co}$$
$$= T_{SWU} + T_{SWO},$$

of throughputs T_{SWU} and T_{SWO}, due to underdense and overdense bursts, respectively.

4.1.2. Selective-Repeat Strategy

Somewhat different approach is used in evaluating the throughput rate for selective-repeat strategy. If we assume that the receiver buffer is infinite and that no errors occur in the feedback channel, the throughput is just equal to the probability that the packet is received correctly [59],

$$T_{SR} = P_c, \qquad (4.1.2-1)$$

representing the average number of packets communicated (i.e., transmitted and received correctly) per transmission. The throughput T_{SR} is obtained as the capacity of an M-ary erasure channel, where M is the number of possible choices for a data packet [46]. Hence, the selective-repeat strategy represents the optimal form of ARQ when the receiver buffer size is unlimited.

The probability of correct packet reception P_c can take on several values. When the beginning of a packet falls within the underdense burst, P_c is equal to P_{cu} from Eq. (3.1.1-3), what happens with the probability

$$P\{P_c = P_{cu}\} = \frac{1}{T_D}\left(\frac{T_D}{t_{IU}}\,\bar{t}_{BU}\right)$$

$$= \frac{\bar{t}_{BU}}{t_{IU}}, \qquad (4.1.2\text{-}2)$$

calculated as the ratio of the total underdense burst time to observation time. $\bar{t}_{BU}$ is the average underdense burst duration. When the packet beginning falls inside an overdense burst, we have that P_c is equal to P_{co} from Eq. (3.1.2-3), what occurs with the probability

$$P\{P_c = P_{co}\} = \frac{1}{T_D}\left(\frac{T_D}{t_{IO}}\,\bar{t}_{BO}\right)$$

$$= \frac{\bar{t}_{BO}}{t_{IO}}, \qquad (4.1.2\text{-}3)$$

calculated as the ratio of the total overdense burst time to observation time. $\bar{t}_{BO}$ is the average overdense burst duration. Elsewhere, P_c is equal to zero.

Total underdense (overdense) burst time is calculated as a product of the expected number of underdense (overdense) bursts in an observation time T_D, and the underdense

(overdense) average burst duration. The mean time between trails is always greater than the average burst duration, in underdense and in overdense case.

Hence, the total probability of a correct packet reception will be

$$P_c = P_{cu} \cdot P\{P_c = P_{cu}\} + P_{co} \cdot P\{P_c = P_{co}\}.$$

Substituting the values from Eqs. (4.1.2-2) and (4.1.2-3), the expression for the selective-repeat throughput becomes

$$T_{SR} = \frac{\bar{t}_{BU}}{t_{IU}} P_{cu} + \frac{\bar{t}_{BO}}{t_{IO}} P_{co}$$
$$= T_{SRU} + T_{SRO}, \qquad (4.1.2-4)$$

the sum of throughputs T_{SRU} and ut T_{SRO}, that are due to underdense and overdense bursts, respectively.

In the derivation of T_{SR} we assumed that a data packet always occupies the spot at the beginning of a burst. Consequently, T_{SRU} is an upper bound on the underdense throughput, since the beginning of an underdense burst is

the most favorable position in the sense of maximizing the probability of a correct packet reception P_{cu}. It is not the situation with the overdense trails, where the probability of correct packet reception P_{co} reaches its maximum sometime within a trail, and T_{SRO} is not an upper bound. On the other hand, P_{co} is always close to or equal to 1. Having that in mind, and the fact that the contribution of overdense trails to the total throughput is small because of their low rate of occurrence, we can consider T_{SR} to be an upper bound on the overall throughput.

4.2. Message Waiting Time

Waiting time to deliver a message, that is in our case a single data packet, is defined as the time elapsed from the moment a transmitter has a packet ready for sending, to the time instant the receiver starts sending back a positive acknowledgment signal.

Underdense and overdense trail arrivals are independent Poisson processes, with respective parameters

$$\lambda_u = \frac{1}{t_{IU}} \quad \text{and} \quad \lambda_o = \frac{1}{t_{IO}}. \tag{4.2-1}$$

The combined random process, consisting of all trail arrivals, is also Poisson with the parameter λ given by

$$\lambda = \lambda_u + \lambda_o, \tag{4.2-2}$$

and, consequently, the mean time between trail arrivals in this new process is

$$\begin{aligned} t_l &= \frac{1}{\lambda} \\ &= \frac{t_{lU}\ t_{lO}}{t_{lU} + t_{lO}}. \end{aligned} \tag{4.2-3}$$

When trail arrivals are modeled as Poisson random points t_i, the message waiting time t_w in a stop-and-wait strategy is defined as

$$\begin{aligned} t_w &= x_{n+1} \\ &= t_{n+1} - t_0. \end{aligned}$$

Quantity x_{n+1} is the time distance from the fixed beginning t_0 of the observation time, i.e., the instant a transmitter has a packet ready for sending, to the $(n+1)$-th random

Poisson point to the right of t_0. Namely, if the number of transmissions required to receive a packet correctly is equal to n, we have to wait till the $(n+1)$-th trail for the receiver confirmation. Random variable x_{n+1} is characterized by Erlang probability density function [42]

$$f_{n+1}(x) = \frac{1}{n!}\lambda^{n+1}x^n e^{-\lambda x},$$

and averaging t_w over x leads to

$$E_x\{t_w\} = \int_0^\infty x_{n+1} f_{n+1}(x)dx$$
$$= \frac{1}{\lambda}(n+1).$$

Furthermore, averaging t_w with respect to n, a discrete random variable representing the number of packet transmissions and defined by Eq. (4.1.1-4), the expected waiting time becomes

$$\bar{t}_w = (1+E)\ t_l$$
$$= \left(1 + \frac{1}{P_c}\right) t_l$$
$$= \left(1 + \frac{1}{P_{cu}P_u + P_{co}P_o}\right) t_l. \qquad (4.2-4)$$

The minimum average waiting time is achieved when each packet is correctly received during its first attempted transmission. Expected number of transmissions E is then equal to 1, and the resulting lower bound on the waiting time to receive a correct packet in a stop-and-wait strategy is

$$\bar{t}_w \geq \bar{t}_{w\min}$$
$$\geq 2t_l, \qquad (4.2-5)$$

a function of communication system parameters only.

4.3. Probability of Correct Message Delivery

4.3.1. Stop-and-Wait Strategy

At times, an important performance measure is the probability of delivering a correct data packet within some specified observation time T_D. For stop-and-wait strategy it can be evaluated as

$$P_D\{t \le T_D\} = \sum_{i=1}^{\infty} P\{C \mid \text{at least i trails in} T_D\} \cdot \cdot P\{\text{at least i trails in} T_D\}.$$

Using the Poisson distribution formula that describes the trail arrivals, the probability P_D becomes

$$P_D\{t \le T_D\} = \sum_{i=1}^{\infty} P_{ci} \prod_{l=1}^{i-1} (1 - P_{cl}) \sum_{k=i}^{\infty} \frac{1}{k!} \alpha^k e^{-\alpha}, \qquad (4.3.1-1)$$

where the summing index i represents the number of necessary transmissions to deliver a packet correctly. P_{ci} and P_{cl} are the total probabilities of correct packet reception during the i-th and l-th transmission. The Poisson process parameter is $\alpha = T_D / t_l$.

Following the argument from Sec. 4.1.1., that total probabilities P_c are statistically independent from trail to trail and have identical values, Eq. (4.3.1-1) simplifies to

$$P_D\{t \le T_D\} = \sum_{i=1}^{\infty} P_c(1-P_c)^{i-1} \sum_{k=i}^{\infty} \frac{1}{k!} a^k e^{-a}. \qquad (4.3.1-2)$$

The second sum in Eq. (4.3.1-2) can be expressed in terms of the chi-square probability function $Q(\chi^2 \mid \nu)$, leading to

$$P_D\{t \le T_D\} = \sum_{i=1}^{\infty} P_c(1-P_c)^{i-1}[1-Q(2a \mid 2i)].$$

This sum can be broken into two parts. The first sum is equal to 1, and in the second sum we will replace the chi-square function by its integral representation, resulting in

$$P_D\{t \le T_D\} = 1 - \sum_{i=1}^{\infty} P_c(1-P_c)^{i-1} \frac{1}{2^i \Gamma(i)} \int_{2a}^{\infty} t^{i-1} e^{-t/2} dt. \qquad (4.3.1-3)$$

Interchanging the order of integration and summation, we have that

$$P_D(t \le T_D) = \frac{1}{2} P_c \int_{2a}^{\infty} e^{-t/2} \sum_{i=0}^{\infty} (1-P_c)^i t^i \frac{1}{2^i i!} dt.$$

Summing over i first,

$$P_D(t \le T_D) = \frac{1}{2} P_c \int_{2a}^{\infty} e^{-t/2} \exp\left[(1-P_c)\frac{t}{2} \right] dt,$$

we obtain the integral that can be solved in a close form. Thus, the probability of delivering the correct packet in at most time T_D is

$$P_D(t \le T_D) = 1 - \exp\left(-\frac{T_D}{t_I} P_c \right), \qquad (4.3.1-4)$$

when stop-and-wait strategy is used.

4.3.2. Selective-Repeat Strategy

The main problem is to determine the amount of available communication time, i.e., the total time the received signal is above some specified threshold. That time is a sum of random underdense and overdense burst durations within the observation time T_D. But the corresponding density function of a sum of random variables representing burst durations could not be found, since the probability density function of either underdense or overdense burst duration is not known in a closed form. Thus, we had to look for an approximate way to calculate the probability of successful packet delivery.

The average number of packets N_p that can be transmitted during some observation time T_D is found as the ratio of the total average communication time to the packet duration T_p [1]

$$N_P = \left\lfloor \frac{1}{T_P}\left(\frac{T_D}{t_{IU}} t_{BU} + \frac{T_D}{t_{IO}} t_{BO}\right)\right\rfloor.$$

---

1 The symbol $\lfloor . \rfloor$ denotes the integer part of the expression.

The total average time available for communication is a sum of the total average underdense and overdense burst times. On the other hand, the total underdense (overdense) burst time is found as a product of the expected number of underdense (overdense) bursts and underdense (overdense) burst duration.

The probability of receiving the correct packet within the time T_D is then

$$P_D(t \le T_D) \le \sum_{i=1}^{N_p} P_c(1-P_c)^{i-1}$$

$$\le 1 - (1-P_c)^{N_p+1}. \qquad (4.3.2-1)$$

where P_c is the total probability of the correct packet reception. Eq. (4.3.2-1) is valid only for $N_p \ge 1$, and represents an upper bound since we assumed that all available slots are used for retransmissions of a single packet.

4.4. Channel Duty Cycle

The duty cycle of a meteor burst communication system is defined as the percentage of time that the received signal is above some arbitrary threshold, what is equivalent to the condition that the trail electron line density be above some minimum value q_{min}. It can be found as the ratio of the total burst time within an observation time T_D, to the observation time T_D itself. On the average, the total burst time is the product of the expected number of trails during the observation time and their mean durations. Taking into account both types of trails

$$\text{duty cycle} = \frac{1}{T_D}\left(\frac{T_D}{t_{IU}}\,\bar{t}_{BU} + \frac{T_D}{t_{IO}}\,\bar{t}_{BO}\right)$$

$$= \frac{\bar{t}_{BU}}{t_{IU}} + \frac{\bar{t}_{BO}}{t_{IO}}, \qquad (4.4-1)$$

where mean values for underdense and overdense burst durations, t_{BU} and t_{BO}, contain the information about the receiver threshold (i.e. q_{min}.) Eq. (4.4-1) is derived assuming that trails of the same or different type do not overlap. If that happens to be the case, it is an upper bound.

5. METEOR BURST CHANNEL CAPACITY

5.1. Gaussian Channel

According to Shannon's coding theorem, the capacity of an additive white Gaussian channel (AWGN) is

$$C = W \log_2\left(1 + \frac{P}{WN_0}\right) \quad \text{bit/s}, \tag{5.1-1}$$

where W is the channel bandwidth, P is the total signal power, and $2W(N_0/2)$ is the total noise power [2]. The formula gives the ultimate limit to transmission rate in a Gaussian channel, and we do not know whether signals used in this work, or any other signals, fall short of this limit.

Strictly speaking, meteor burst channel is not an AWGN channel, since its noise power spectral density from Eq. (2.1.10-1) is a function of frequency. But if we confine our signals into the narrow bandwidth around the carrier frequency, as it is the case with BPSK modulation that is

used in this work, the value of N_0 inside that bandwidth will not change much compared to its nominal value at the carrier frequency, and we can assume that N_0 is constant.

Similar reasoning is valid for the received signal power. Constants in transmission equations for underdense and overdense trails, Eqs. (2.1.2-2) and (2.1.3-2), respectively, are also functions of frequency, but their values do not change significantly inside the narrow BPSK signal bandwidth. It means that values of the received power need no correction for the frequency fall-off.

Instantaneous channel capacity from Eq. (5.1-1) is a function of the random power P, received from underdense and overdense trails. Received power is a function of several random variables: trail arrival times, electron line densities of underdense and overdense trails, and power decay constant of underdense trails. To find the average channel throughput,

$$E\{T\} = \frac{W}{\ln 2}\, E\left\{\ln\left(1 + \frac{P}{W N_0}\right)\right\},$$

we will use the result from theory of convex functions, stating that [54]

$$E\{f(x)\} \leq f(E\{x\}),$$

when $f(x)$ is a convex cap function. The capacity function satisfies this condition, since its second derivative with respect to P is less than zero for all values of P. Thus,

$$E\{T\} \leq \frac{W}{\ln 2} \ln\left(1 + \frac{1}{WN_0} E\{P\}\right), \tag{5.1-2}$$

where $E\{P\}$ is the total average power received from underdense and overdense trails. In order to find the average throughput, we will deal separately with aforementioned random variables.

The number $n(t_1,t_2)$ of Poisson points t_i in the interval (t_1,t_2) of the length $t=t_2-t_1$ is a random variable. The probability that exactly k Poisson points fall into the interval (t_1,t_2) is equal to

$$P\{n(t_1,t_2)=k\} = \frac{(\lambda t)^k}{k!}\, e^{-\lambda t}.$$

Using the Poisson points t_i we form a new stochastic process, defined as

$$x(t) = n(0,t),$$

representing the number of Poisson points in the interval $(0,t)$. This is a discrete state process consisting of increasing staircase functions with discontinuities at the points t_i. If we bring the Poisson process $x(t)$ to the input of a differentiator, the output will be a train of Poisson impulses

$$z(t) = \sum_i \delta(t-t_i). \qquad (5.1-3)$$

In particular, using the values for λ from Eq. (4.2-1), we will have that

$$P\{n_u(t_1,t_2)=k\} = \frac{(\lambda_u t)^k}{k!}\, e^{-\lambda_u t},$$

and

$$P\{n_o(t_1,t_2)=k\} = \frac{(\lambda_o t)^k}{k!}\, e^{-\lambda_o t},$$

where $n_u(t_1,t_2)$ and $n_o(t_1,t_2)$ are numbers of underdense and overdense trails in the interval (t_1,t_2), respectively. In that sense, we form the process

$$z_u(t) = \sum_i \delta(t-t_{iu}),$$

representing the arrivals of underdense trails, and the process

$$z_o(t) = \sum_j \delta(t-t_{jo}),$$

that represents the arrivals of overdense trails. Instants t_{iu} and t_{io} are the arrival times of underdense and overdense trails, respectively.

The total power received from the meteor burst channel is then

$$P(q_1,q_2,b;t) = z_u(t)*P_{su}(q_1,b;t) + z_o(t)*P_{so}(q_2;t), \tag{5.1-4}$$

evaluated as the convolution of processes $z_u(t)$ and $z_o(t)$, and powers $P_{su}(q_1,b;t)$ and $P_{so}(q_2;t)$ received from underdense and overdense trails, respectively. The underlying assumption here is that underdense and overdense trail arrivals are independent stochastic processes, and that trails do not overlap in time. (If trails do overlap, Eq. (5.1-4) represents an upper bound.) Performing the convolution from Eq. (5.1-4), the received power expression becomes

$$P(q_1,q_2,b;t) = \sum_i P_{su}(q_1,b;t-t_{iu}) + \sum_j P_{so}(q_2;t-t_{jo}).$$

Averaging $P(q_1,q_2,b;t)$ from Eq. (5.1-4) with respect to random variables representing trail arrivals,

$$E\{P(q_1,q_2,b;t)\} = P_{su}(q_1,b;t)*E\{z_u(t)\} + \\ + P_{so}(q_2;t)*E\{z_o(t)\},$$

and having in mind that expected values of stationary processes $z_u(t)$ and $z_o(t)$ are

$$E\{z_u(t)\} = \lambda_u \quad \text{and} \quad E\{z_o(t)\} = \lambda_o,$$

we end up with

$$E\{P(q_1, q_2, b; t)\} = \lambda_u \int_0^{\infty} P_{su}(q_1, b; t)dt + \lambda_o \int_0^{aq-k} P_{so}(q_2; t)dt.$$

The thing to do next is to integrate the underdense received power over the underdense burst duration,

$$\int_0^{\infty} P_{su}(q_1, b; t)dt = C_u q_1^2 \int_0^{\infty} \exp\left(-\frac{t}{b}\right)dt$$

$$= C_u q_1^2 b.$$

We took here that the duration of an underdense burst is infinite, although it really is equal to t_{BU} from Eq. (2.1.7-1), but this approximation brings insignificant changes to the final result. Furthermore, integrating the overdense received power over the overdense burst duration, we get

$$\int_0^{aq_2-k} P_{so}(q_2;t)dt \cong \sqrt{\frac{2\pi}{27}} C_o a q_2 \sqrt{a q_2}.$$

The last integral is approximated using the Formula (4.269-3) from [17]. We again neglected here the fact that effective duration of a burst, in communication terms, may be shorter than assumed by integration limits. Virtual burst duration is a function of the received power threshold, imposed either by the receiver sensitivity or by the desired maximum bit error probability in transmission that we want to maintain. This approximation is validated by the fact that we are looking for an upper bound on throughput, independent of the user selected threshold.

The final result of averaging the received power over random trail arrivals is then

$$E\{P(q_1,q_2,b)\} = \frac{1}{t_{IU}} C_u b q_1^2 + 0.48 \frac{1}{t_{IO}} C_o a q_2 \sqrt{a q_2}.$$

Averaging the power $P(q_1,q_2,b)$ further over electron line densities q_1 and q_2, and decay constant b,

$$E\{P\} = \frac{C_u}{t_{IU}} \int_{b=0}^{\infty} \int_{q_1=q_{minu}}^{q_{uu}} b q_1^2 f(b) f(q_1) db\, dq_1 +$$

$$+ \frac{0.48}{t_{IO}} C_o a \int_{q_2=q_{minuo}}^{q_{uo}} q_2 \sqrt{a q_2} f(q_2) dq_2,$$

we obtain the final expression for average power in the form

$$E\{P\} = 0.7 \frac{1}{t_{IU}} C_u Q_1 \bar{b} \; (q_{uu}^{1.4} - q_{minu}^{1.4}) +$$

$$+ 0.48 \frac{1}{t_{IO}} C_o Q_2 a^{1.5} (q_{uo} - q_{mino}).$$

Substituting this result in Eq. (5.1-2), we obtain an upper bound on the average meteor burst channel throughput as

$$\bar{T} \leq \frac{W}{\ln 2} \ln[1 + \frac{0.7}{W N_0 t_{IU}} C_u Q_1 \bar{b} \; (q_{uu}^{1.4} - q_{minu}^{1.4}) +$$

$$+ \frac{0.48}{W N_0 t_{IO}} C_o Q_2 a^{1.5} (q_{uo} - q_{mino})]. \qquad (5.1-5)$$

This is a general bound, valid also in case of ARQ transmission, since Shannon proved that channel capacity is not increased by introduction of feedback [46].

5.2. Binary Symmetric Channel

More realistic values for the throughput are obtained if we consider the meteor burst channel to be a binary symmetric channel (BSC). In general, the BSC capacity is

$$C = 1 + p \cdot \log_2 p + (1-p) \cdot \log_2 (1-p) \quad \text{bits/bit},$$

where p is a channel bit error rate. For underdense trails and BPSK modulation, the conditional bit error rate is given by

$$p_u = P_{bu}(q_1, b; t)$$
$$= \frac{1}{2} \, erfc \sqrt{\frac{C_u q_1^2}{N_0 R} \exp\left(-\frac{t}{b}\right)},$$

following the reasoning from Sec. 3.1.1. For overdense trails, and the same type of modulation, bit error rate is

$$p_o = P_{bo}(q_2;t)$$

$$= \frac{1}{2}\ erfc\left(\frac{C_o}{N_0 R}\sqrt{(k+t)\ \ln\left(\frac{aq_2}{k+t}\right)}\right)^{\frac{1}{2}},$$

this time following the development from Sec. 3.1.2. We can consider the meteor burst channel throughput to be a random variable, taking values

$$T = \left\{\begin{matrix} T_u, & \text{during underdense bursts,} \\ T_o, & \text{during overdense bursts,} \\ 0, & \text{elsewhere.} \end{matrix}\right\}$$

In the long run, the probability that throughput T will be equal to T_u is

$$P\{T = T_u\} = \frac{\bar{t}_{BU}}{t_{IU}},$$

evaluated as the ratio of the total underdense burst time to the observation time, as in Eq. (4.1.2-2). Similarly, the throughput T will take the value T_o with probability

$$P\{T = T_o\} = \frac{\bar{t}_{BO}}{t_{IO}},$$

calculated this time as the ratio of the total overdense burst time to observation time, as in Eq. (4.1.2-3). The average throughput is then found as

$$\bar{T} = \frac{\bar{t}_{BU}}{t_{IU}} [1 + p_u \cdot \log_2 p_u + (1 - p_u) \cdot \log_2 (1 - p_u)] +$$

$$+ \frac{\bar{t}_{BO}}{t_{IO}} [1 + p_o \cdot \log_2 p_o + (1 - p_o) \cdot \log_2 (1 - p_o)].$$

The values for bit error probabilities p_u and p_o change with time t elapsed from the beginning of a trail, and they will be at their minimum when the received power is maximum. For underdense trails it happens for time $t = 0$, and the corresponding minimum underdense bit error probability is

$$p_{u\,min} = P_{bu}(q_1, b; 0)$$

$$= \frac{1}{2} \, erfc \sqrt{\frac{C_u q_1^2}{N_0 R}}.$$

For overdense trails, the received power is at its maximum when time is equal to

$$t = \frac{aq_2}{e} - k,$$

and the minimum overdense bit error probability is

$$p_{o\,min} = P_{bo}\left(q_2; \frac{aq_2}{e} - k\right)$$

$$= \frac{1}{2}\, erfc\left(\frac{C_o}{N_0 R}\sqrt{\frac{aq_2}{e}}\right)^{1/2}.$$

Using the conditional probabilities $p_{u\,min}$ and $p_{o\,min}$, we calculate the corresponding total probabilities $P_{u\,min}$ and $P_{o\,min}$ as

$$P_{u\,min} = \int_{b=0}^{\infty} \int_{q_1=q_{min\,u}}^{q_{up}} p_{u\,min} f(b) f(q_1) dq_1 db,$$

and

$$P_{o\min} = \int_{q_2 = q_{mino}}^{q_{uo}} p_{o\min} f(q_2) dq_2 .$$

Throughput is at its maximum when the bit error probability is minimum, and we obtain the upper bound on the average throughput of a binary symmetric meteor burst channel as

$$\overline{T} \leq \frac{\bar{t}_{BU}}{t_{IU}} [1 + P_{u\min} \cdot \log_2 P_{u\min} + (1 - P_{u\min}) \cdot \log_2 (1 - P_{u\min})] +$$

$$+ \frac{\bar{t}_{BO}}{t_{IO}} [1 + P_{o\min} \cdot \log_2 P_{o\min} + (1 - P_{o\min}) \cdot \log_2 (1 - P_{o\min})]. \quad (3.4-6)$$

This bound is also valid for ARQ transmission, as concluded in Sec. 5.1.

6. SIMULATION AND RESULTS

6.1. The Sample System

Results from calculations and simulations that are presented in this chapter are for the specific sample system, chosen as the representative of the systems currently used in meteor burst communications. Parameter values are as follows:

$P_T = 1000\ W$	Transmitter power
$G_T = G_R = 10\ dB$	Transmitter and receiver antenna gains
$L = 1000\ km$	Communication link distance
$R_T = R_R = 514\ km$	Transmitter and receiver distances from a meteor trail
$f = 50\ MHz$	Transmitter carrier frequency
$\lambda = 6\ m$	Carrier wavelength
$\phi = 153.12°$	Angle between radii R_T and R_R
$D = 8\ m^2/\text{sec}$	Diffusion constant
$\zeta = 45.84°$	Antenna beamwidth
$P_{b\,max} = 10^{-4}$	Maximum allowed bit error rate

For those parameters, values for constants from statistical models are:

$N_0 = 4.89 \times 10^{-20}\ W/Hz$	Noise power spectral density
$C_u = 3.81 \times 10^{-42} W$	Underdense power constant
$C_o = 2.37 \times 10^{-13}\ W$	Overdense power constant
$k = 0.013$ sec	"
$\alpha = 5.95 \times 10^{-15}$ sec	"

6.2. Simulation

In order to gain more insight into the transmission properties of the meteor burst channel, and to verify some of the calculated performance characteristics, a computer simulation program was developed according to the probabilistic model of the channel outlined in Chapter 2. IMSL Software Library of mathematical and statistical subroutines was used in the implementation of the simulator [28].

The simulation allows for transmission of arbitrary length packets with fixed data rate of up to R_{maxu}, the maximum data rate attainable using underdense trails and BPSK modulation, given by

$$R_{maxu} = \frac{C_u \, q_{uu}^2}{N_0[erfc^{-1}(2P_{bmax})]^2},$$

or, alternately, up to R_{maxo}, the maximum data rate for overdense trails

$$R_{maxo} = C_o\sqrt{\frac{aq_{uo}}{e}} \; \frac{1}{N_0[erfc^{-1}(2P_{bmax})]^2}.$$

Inputs to the program are observation time, maximum desired bit error rate P_{bmax}, transmission data rate, and number of bits per packet. Observation time can be set to the maximum of 6 hours, what will determine the number of underdense and overdense trails available for transmission. The value for P_{bmax} is used to set the receiver threshold, according to Eq. (2.1.4-3).

Random number generator is used to produce bit values for packets of desired length, which are then stored into the transmitter buffer. If coding is used, information bits are passed through the convolutional encoder before storage. Code rate can be set to 1/2 or 1/3, constraint length may have values of up to 7, and the decoder is provided with the memory length of up to 70 bits. Code generators are from the table of optimum short constraint length convolutional codes [40].

Trail arrival times are generated using Poisson random deviate generator, with Poisson parameters for underdense and overdense trails defined in Eqs. (2.1.9-2) and (2.1.9-3). Random deviates for electron line densities and decay constant are generated following the cumulative distribution functions given by Eqs. (2.1.4-2), (2.1.5-2), and (2.1.6-2). Samples of Gaussian noise have power spectral density from Eq. (2.1.10-1).

In the correlation receiver, hard decision is brought upon individual bits according to the signal sample calculated from received power, Eqs. (2.1.1-1) and (2.1.3-1), and noise. Bit values are then stored in the receiver

buffer. In case of coded transmission, the received packet is first decoded by the maximum-likelihood Viterbi algorithm. The packet in the receiver buffer is checked for errors, and appropriate acknowledge signal is issued. If the packet is correct, ACK signal causes the transmission of a new packet, and if errors are found the same packet is retransmitted over the first available trail. At the end of the observation time, throughput and waiting time are calculated from the accumulated statistics about the number of packets transmitted, number of retransmissions, and times elapsed from the first transmission of each of the packets and the reception of a positive acknowledgment signal.

6.3. Results

Since close form expressions for most of the performance characteristics could not be obtained in a closed form, statistical averages were calculated numerically with the help of integration subroutines from the IMSL package.

6.3.1. Stop-and-Wait Strategy

Throughput rate for uncoded transmission as a function of data rate R is shown in Fig. 1, with the number of information bits per packet as a parameter. Throughput values are calculated according to Eqs. (4.1.1-14), (3.1.1-3), and (3.1.2-3). For relatively short packets (N = 100, 500, and 1000 bits,) the throughput decreases monotonically with increase in the data rate, and no optimum data rate is observed. The main reason for the decrease in throughput is the increase in the number of idle bit times, i.e., the increase in the mean time between trail occurrences. The mean time between underdense bursts, which are the dominant propagation medium at low data rates, is 2.25 seconds at 1 kbit/sec and goes to 8.62 seconds at 10 kbits/sec. Mean time between overdense bursts is about 150 seconds, remaining at that value up to 100 kbits/sec, and their influence on throughput in this sample system and for this channel model is a second order effect. The maximum in throughput curve shows only for longer packets. At low data rates their length often exceeds the burst length, the probability of receiving the packet correctly becomes low, and the drop in throughput results.

The average burst duration at 1 kbit/sec is 0.6 seconds and falls to 0.36 seconds at 10 kbits/sec. For a fixed packet size of N bits, a drop in throughput will happen when the packet duration $T_p = N/R$ becomes much greater than the average burst length. This consideration is more readily seen from Fig. 2, where uncoded throughput values are plotted versus the packet size, with bit rate as a parameter. At a constant data rate, throughput is small for short packets, and rises steadily as the number of bits per packet is increased. The maximum is reached around 700 bits at 1 kbit/sec, and 1300 bits at 2 kbits/sec, showing that the optimum packet length is slightly greater than the average burst length. Further increase in packet length brings no benefit but rather decrease in throughput, what is the consequence of the rise in the number of packet retransmissions. As the received power falls exponentially with the time measured from a burst formation, long packets experience unfavorable signal-to-noise ratios most of the time. Lower throughput maxima, as the data rate R increases, are due to the aforementioned fact of the growing number of idle bit times.

Waiting time to receive an error-free packet, defined in Sec 4.2., is plotted in Fig. 3 versus the packet size, with bit rate as a parameter. At a given data rate, the shorter the packet the lower will be the probability of an error event. The number of retransmissions is subsequently decreasing what, in turn, reduces the waiting time to receive a positive acknowledgment signal from the receiver. The only effect that could be observed here is a steep rise in the waiting time for very low bit rates and long packets. Again, it is the consequence of packet duration greatly exceeding the average burst length. Crossing points of curves determine the intervals of more or less favorable combinations of data rates and packet sizes that minimize the waiting time. For example, if our packets are up to 1000 bits long we should transmit at 1 kbit/sec, and beyond that we are better off with the increase in the transmission rate.

Fig. 4 points to an important observation that optimum transmission rate exists for every packet length, in terms of minimizing the waiting time. Comparing Figs. 2 and 4, we see that we can almost simultaneously optimize the throughput and the waiting time. The minima are pretty

broad for all packet sizes, meaning that the choice of transmission speed is not too limited, except for longer packets, when lowering the speed can bring sharp increase in waiting time. Thus, it is always better to operate at slightly higher than optimum data rate. The curves show general increase in waiting time as data rates become higher, what is the consequence of the rise in trail interarrival times. The bottom curve in Fig. 4 represents the minimum achievable average waiting time to deliver a packet of data, as defined in Eq. (4.2-5). That would happen in the case of every packet being received correctly the first time it is transmitted.

Idle times between bursts, and the limiting factor of the usable burst portions in communication terms, are the physical phenomena that cannot be overcome. The other major cause of delays in delivering a message to the recipient, and of relatively modest amount of achieved throughput, is the number of retransmissions of any single packet. The expected number of retransmissions is inversely proportional to the average probability of a packet being error free, as noted in Eq. (4.1.1-10). Thus, the way to overcome system shortcomings is to increase the probability of

correct packet reception. That led us to try hybrid ARQ schemes where, in addition to the feedback channel, forward error correction is employed.

Behavior similar to the one described in connection with Figs. 1 to 4 is observed for all hybrid FEC-ARQ schemes. Packets were convolutionally encoded with rate-1/2, rate-3/4, and rate-7/8 codes. Rather than repeating the performance curves for every code rate, the impact of FEC-ARQ schemes is summarized in Figs. 5 and 6.

Fig. 5 offers the comparison of throughput rates for uncoded and coded transmission. Rate-1/2 code yielded no improvement, and rate-3/4 code was beneficial to certain extent for some of the packet lengths. The real advantage of coding is seen only when code rates approach to 1, where throughput is increased for all packet sizes of interest. The data rate parameter in all cases was 1 kbit/sec, as it provides for the maximum throughput.

The comparison of waiting times for uncoded case, low-rate code (rate-1/2), and high-rate code (rate-7/8), is shown in Fig. 6. We see that high-rate codes yield lower

waiting times at all data rates, when compared to the uncoded case. Low-rate codes become superior to uncoded transmission as data rate increases, but then the throughput is prohibitively low. The other disadvantage of low-rate codes is that their waiting times increase sharply for low data rates, just when the throughput is at its maximum.

In Fig. 7, the probability of correct packet reception is plotted against the observation time, for the uncoded case and rate-1/2 and rate-7/8 codes. Here again high-rate codes are advantageous, leading to higher probabilities of correct packet reception, regardless of the observation time.

6.3.2. Selective-Repeat Strategy

In this ARQ scheme we concentrated on short packets, as it is known that selective-repeat throughput increases with decrease in the packet size. There exists no optimum block length that maximizes the selective-repeat throughput, neglecting the trivial case of block length equal to 1, as proven in [38]. In practice, the smallest block length allowed is the best choice, having in mind

that real systems always require some minimum overhead.

The value for selective-repeat throughput in Eq. (4.1.2-4) is difficult to calculate precisely, because of the complexity involved in the computation of correct packet reception. The position of a specific packet inside the trail is a random variable whose values are known. They are discrete time instants separated by a packet length, but their probabilities are influenced by many factors whose contributions are not easy to state analytically. We can assume that the distribution is uniform, but even then integrations become involved and time consuming, and we evaluated bounds rather than exact expressions.

Fig. 8 represents the comparison of throughput rates for uncoded ARQ and various FEC-ARQ schemes. For very short packets FEC-ARQ does not bring improvement, but such packets may be impractical in real transmission systems. Rate-1/2 codes are not beneficial at any packet length. With increase in packet size all other code rates provide for increase in throughput, as compared to uncoded transmission, with increase being larger as the code rate approaches to 1. The overall throughput falls-off monotonically for longer

packets as expected, since the probability of losing the last packet in the trail is rising. All throughput values ar calculated as upper bounds on the actual throughput, assuming that the particular packet always finds itself positioned at the beginning of a burst. Simulation results show that the actual throughput is about 70 percent of the calculated upper bound.

The question now arises about the feasibility of a selective-repeat scheme, since it is optimum only in the case of infinitely long buffers. To estimate practical buffer size, capable of sustaining the throughput predicted in Fig. 8, we will use the notion of the block storage of the link. The number of blocks S stored by the link is [59]

$$S = \left\lceil \frac{R(3t_{emis} + 2t_{prop})}{N} \right\rceil.$$

R is data rate, $T_{emis} = N/R$ is the emission delay of an N-bit block transmitted at data rate R, and t_{prop} is the propagation

delay.[1] Since the data link stores S blocks, selective-repeat scheme must employ a receiver capable of storing at least S blocks. Otherwise blocks cannot be delivered continuously, in a correct order, following an error. On the other hand, if we provide the receiver with a buffer of size qS blocks, the buffer overflow will occur only after q attempts to send a copy of a block in error have failed. For example, in case of $N = 100$ bits per packet, data rate of 1 kbit/sec, and 1000 km link, the link storage is $S = 4$ blocks. Simulation showed that 2.29 retransmissions are needed, on the average, to communicate a block successfully. The required buffer capacity is thus 12 blocks, what shows that estimated throughput could be maintained with a relatively modest buffer size.

Feasibility of selective-repeat ARQ scheme is even less in question when computer-to-computer communications are concerned. Large amounts of high-speed and low-speed storage available allow for transmission of much larger packets, since blocks of data can easily be sorted if

---

1 The notation $\lceil x \rceil$ signifies the smallest integer greater than or equal to x.

received out of order. Sorting is achieved by re-sequencing block storage addresses, and no movement of data is really necessary [6].

As for the probability of correct packet reception, the same conclusion is valid here as in the stop-and-wait protocol: High-rate codes are advantageous, leading to higher probabilities of correct packet reception, regardless of the observation time.

6.3.3. Channel Capacity

Upper bound on the average throughput of a meteor burst channel, as a function of transmission rate, is shown in Fig. 9. The meteor burst channel is here regarded as a binary symmetric channel. The decrease in throughput with increase in data rate is the consequence of the rise in trail interarrival times. It is assumed that usage of the channel is attempted at all times, not only when we know that the trail exists. In addition, an upper bound on the average meteor burst channel throughput is shown in Fig. 10, as a function of channel bandwidth. This time the meteor burst channel is regarded as an AWGN channel.

7. CONCLUSION

The goal of this work was to examine the performance characteristics of an ARQ communication system, operating over a meteor burst channel. The problem was approached from two sides. Early in the work we became aware that closed form solutions are not something we could expect. Turning to simulation seemed more promising, and in fact gave us more feeling about the nature of phenomena involved in the communication process. Enriched with this insight we could look back to analytical derivations with more realistic expectations.

Simulations and calculations were done on the basis of the statistical model of a meteor burst channel. The model itself is based on the classical power transmission equations describing two main and distinct phenomena in the channel, underdense and overdense trails. Second order effects, like sporadic-E and auroral scatter, were not included in the model, and we concentrated our effort on stochastic parameters we concluded were crucial. Distribution functions for underdense and overdense electron line densities are based on experimental data from radio and

radar observations of the channel, and include recent findings. Decay constant for underdense trails is taken to be Rayleigh distributed, although some authors prefer the exponential distribution. Trail arrivals are modeled as a Poisson process, and expressions for the mean time between arrivals are a mixture of basic electromagnetic considerations and practical observations. Geographic, seasonal, and daily variations in all mentioned parameters were not included in the model for two reasons. First, we wanted to keep the simulation model as simple as possible, since the computations become costly and involved with introduction of many random variables; and second, too few experimental data were publicly available to gain general insight and indicate the way of implementing them into the simulation. Only noise of galactic origin and the one generated in the receiver were taken into account, neglecting the sometimes predominant effect of a man made noise. But the fact is that all today's operational meteor burst communication systems are installed in remote sites, where nonnatural interference is very unlikely. In addition, the results are obtained for a sample system we believe is a good representative of the systems currently used in practice.

In this light, the conclusions drawn from the results of calculation and simulation are only as good as the model is. Its general application is not clear, since we could well see relatively large differences among the data obtained from different links. Not going into particularities, we could say that results obtained conform, in general, with published conclusions about the behavior of a meteor burst channel.

The simulation program developed offers enough flexibility to be used for testing various modulation types, coding schemes, and communication protocols, under a wide range of system and link parameters. Going as far as it was possible into analytical derivations, we indicated ways to calculate the performance characteristics by numerical evaluation of statistical averages, and obtained good accordance between calculated and simulated results.

Throughput rate, waiting time to receive a message correctly, and probability of receiving a message within the specified time, were chosen as the main performance measures, since they are strongly related to the communication protocol used. Duty cycle, on the other side, is

predominantly a function of channel characteristics and communication system parameters, independent of the protocol used. As for the channel capacity, an upper bound in the Shannon's sense was obtained, to serve more as the ultimate goal than something achievable in practice. In addition, an upper bound on the channel capacity is derived, when meteor burst channel is regarded as a binary symmetric channel.

We estimated the performance of an ARQ communication system transmitting BPSK data at a constant data rate, under two protocols: stop-and-wait and selective-repeat. We also looked into the possible benefits of hybrid FEC-ARQ schemes which, in addition to feedback, offer some degree of error correction.

It is found that, in both coded and uncoded stop-and-wait strategy, there exists an optimum packet length for every data rate, in terms of minimizing the waiting time and maximizing the throughput. The packet duration should be slightly larger than the average burst length of underdense trails. Convolutional encoding of packets improves the throughput and probability of correct packet reception,

decreasing at the same time the expected message waiting time, but only when high-rate codes are employed. Improvements are higher as the code rate approaches to 1. Low-rate codes have mostly the opposite effect, and degrade the system performance.

In a selective-repeat strategy, short packets offer the highest throughput as expected, and at that point coded and uncoded schemes have identical performance. The benefit of using high-rate codes shows with the increase in packet size. The longer the original packet, and the closer the code rate is to 1, the larger the improvement in throughput will be, as compared to uncoded transmission. Both coded and uncoded throughput are generally higher in selective-repeat strategy.

Our results have been confirmed by recent experimental data from high latitude meteor burst channel, showing that it is much easier to deliver many short messages than a few long ones [7]. Although different type of coding was used, the conclusion is identical to the one obtained in this work: Small amount of forward error correction improves ARQ performance, and the use of codes seems limited to high

rate ones. Low rate codes can correct more errors, but additional parity bits become self-defeating under the strong constraint of finite burst length. Yet another empirical analysis of forward error correction in meteor burst communication is in accordance with our conclusion, the only difference being again the use of BCH codes [11]. It demonstrated increase in throughput and decreased delays with respect to delivery of short messages, when using simple FEC techniques and code rates as close to 1 as possible.

8. FIGURES

FIG. 1
THROUGHPUT RATE
STOP--AND--WAIT STRATEGY
(UNCODED TRANSMISSION)

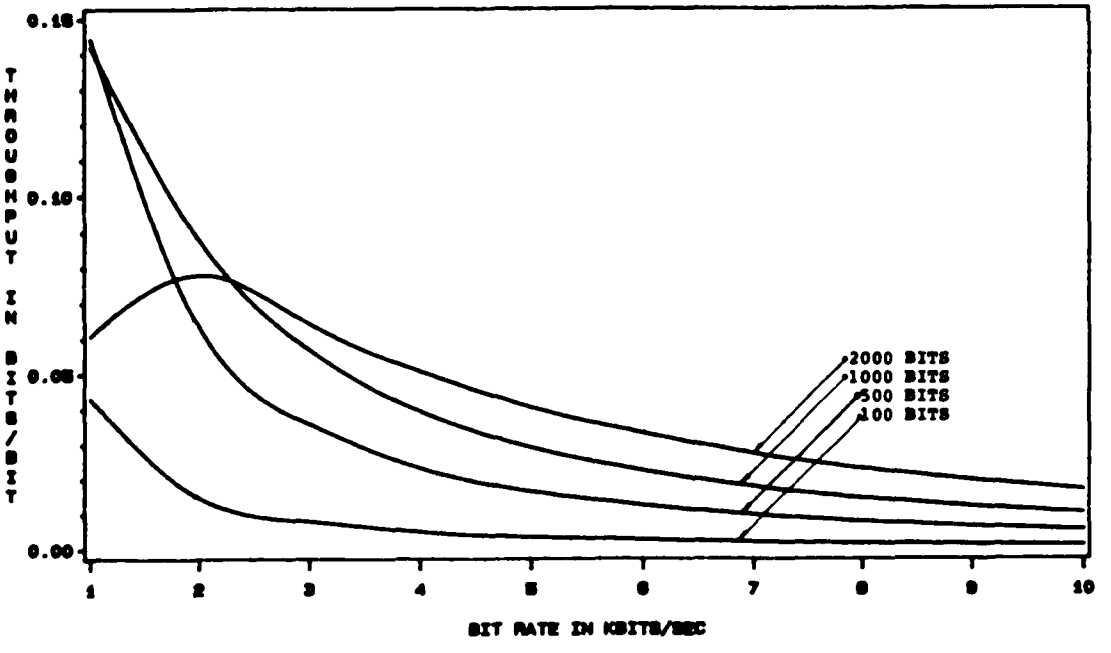

FIG. 2
THROUGHPUT RATE
STOP-AND-WAIT STRATEGY
(UNCODED TRANSMISSION)

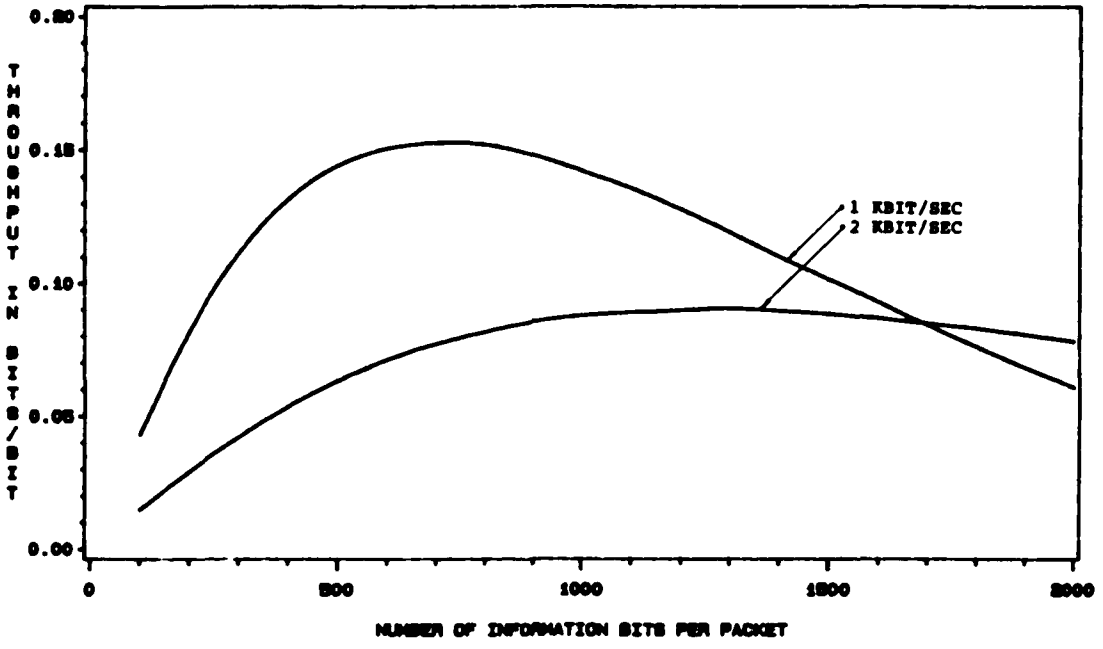

FIG. 3
WAITING TIME TO RECEIVE A PACKET
STOP-AND-WAIT STRATEGY
(UNCODED TRANSMISSION)

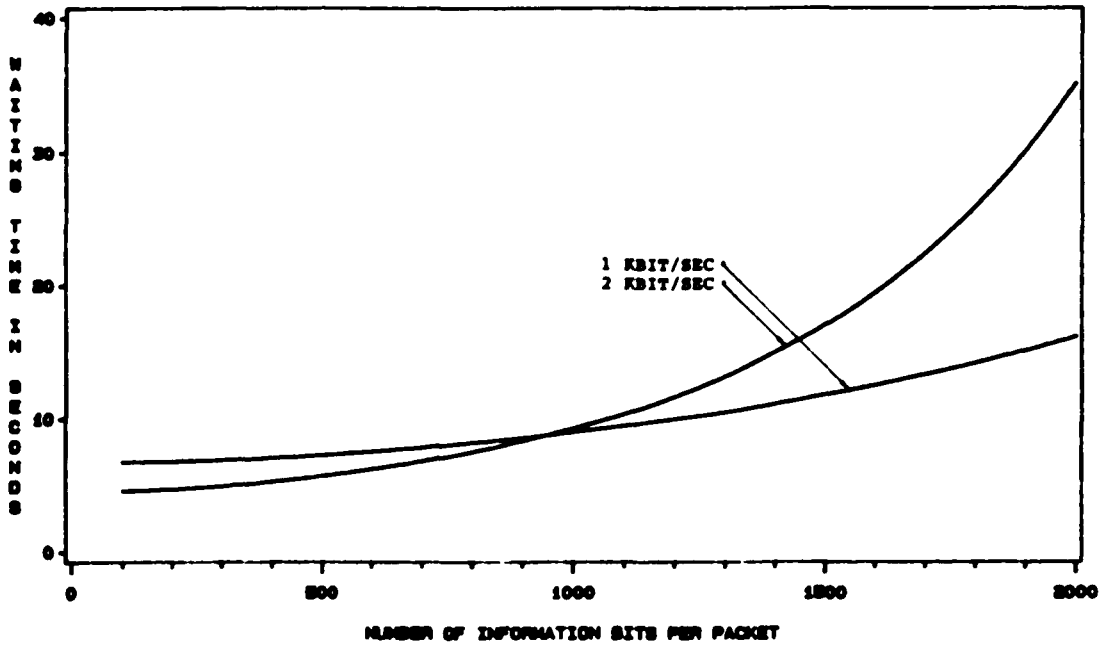

FIG. 4
MESSAGE WAITING TIME
STOP-AND-WAIT STRATEGY
(UNCODED TRANSMISSION)

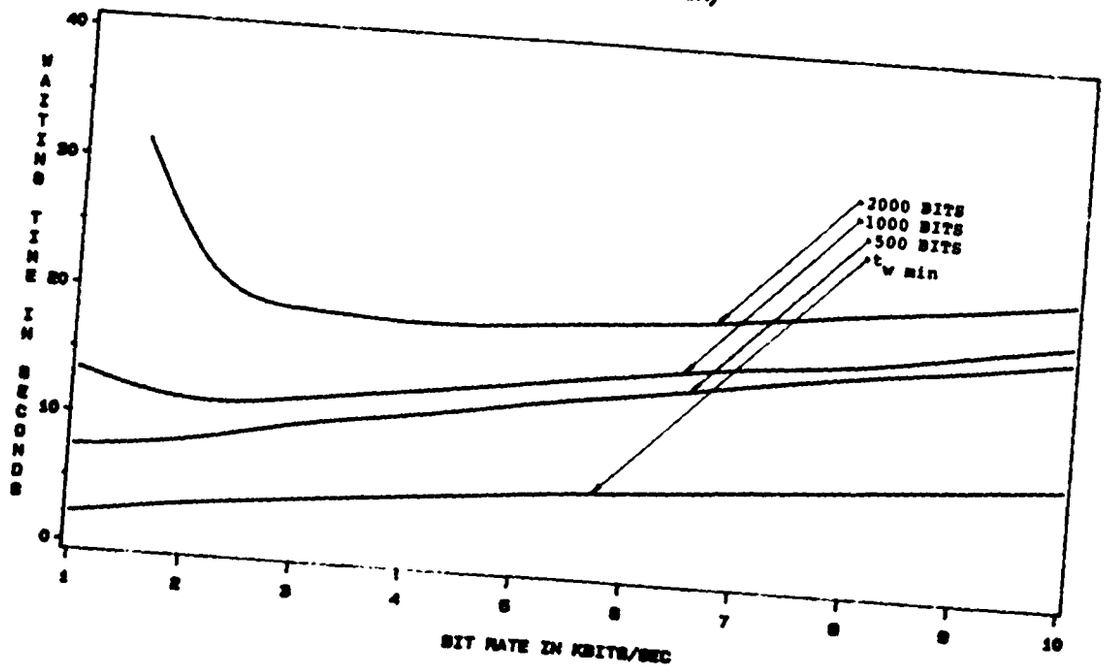

FIG. 8
THROUGHPUT RATE
COMPARISON OF CODED AND UNCODED TRANSMISSION
STOP-AND-WAIT STRATEGY
(DATA RATE R = 1 KBIT/SEC)

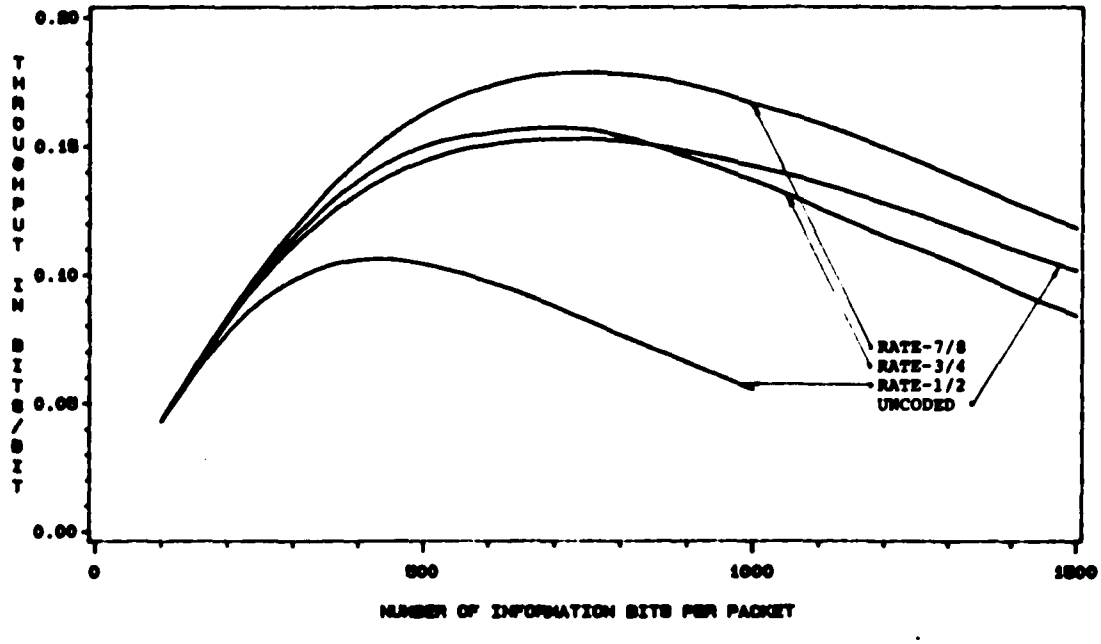

FIG. 6

WAITING TIME TO RECEIVE A PACKET

COMPARISON OF CODED AND UNCODED TRANSMISSION
STOP-AND-WAIT STRATEGY
(1000 INFORMATION BITS PER PACKET)

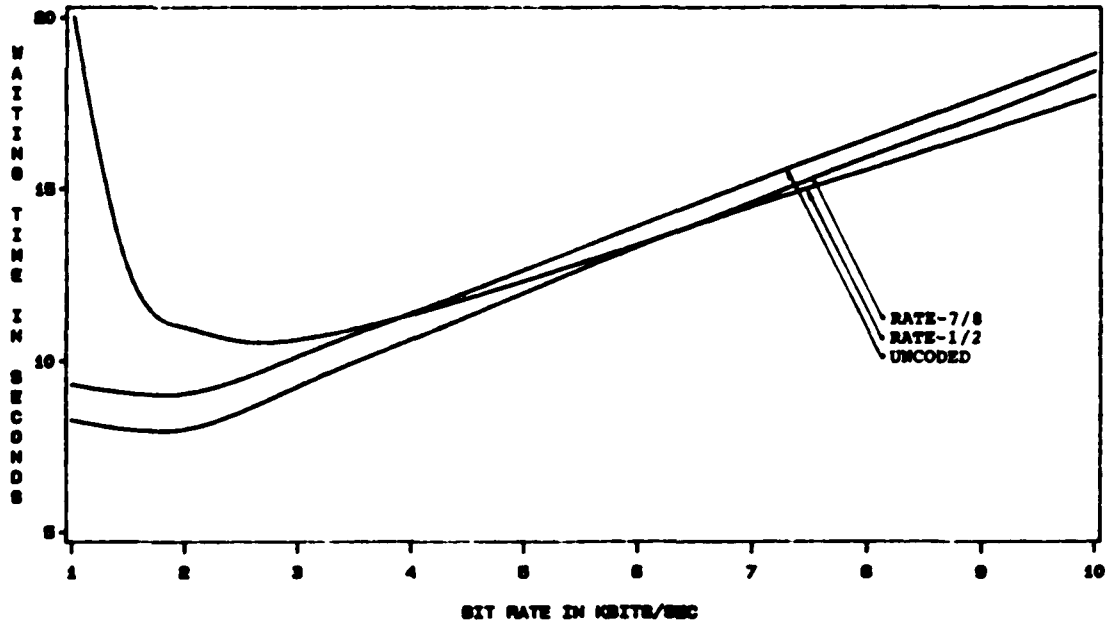

FIG. 7
PROBABILITY OF CORRECT PACKET RECEPTION
STOP-AND-WAIT STRATEGY
(BIT RATE: 1 KB/S, PACKET LENGTH: 700 BITS)

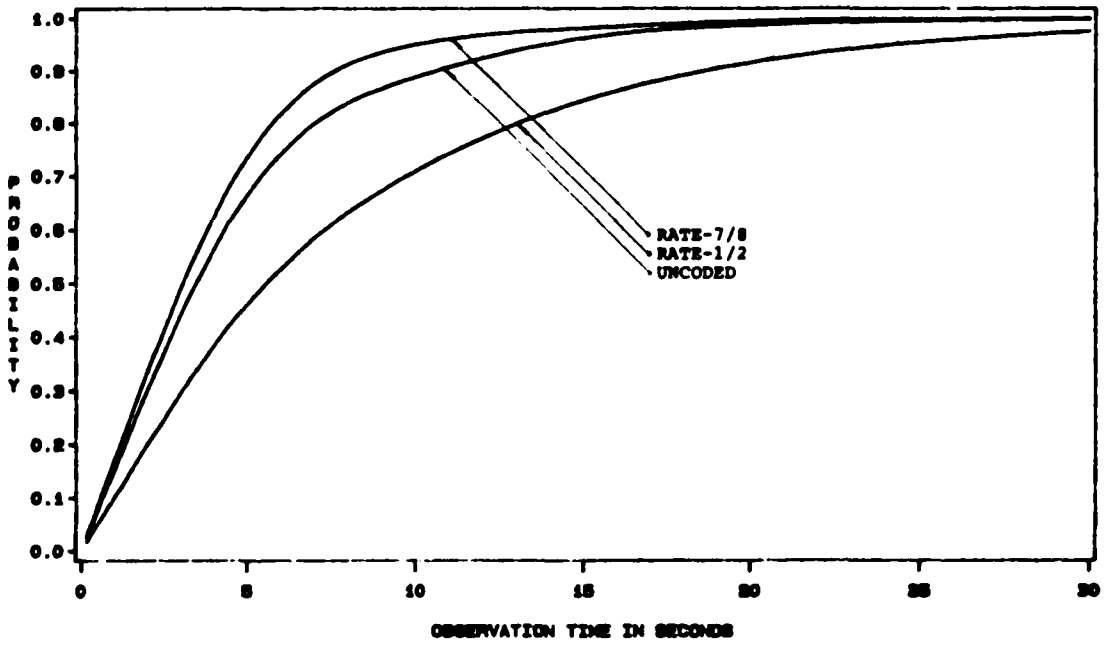

FIG. 8
THROUGHPUT RATE
COMPARISON OF CODED AND UNCODED TRANSMISSION
SELECTIVE-REPEAT STRATEGY
(BIT RATE 1 KBIT/SEC)

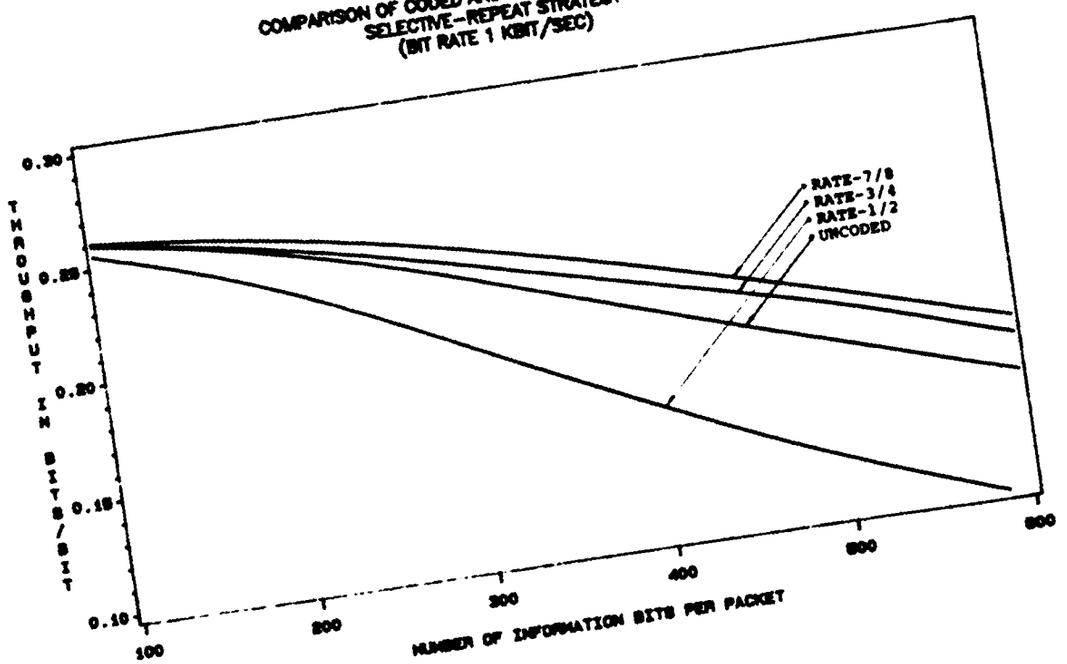

FIG. 9
AVERAGE THROUGHPUT RATE FOR BSC CHANNEL
(UPPER BOUND)

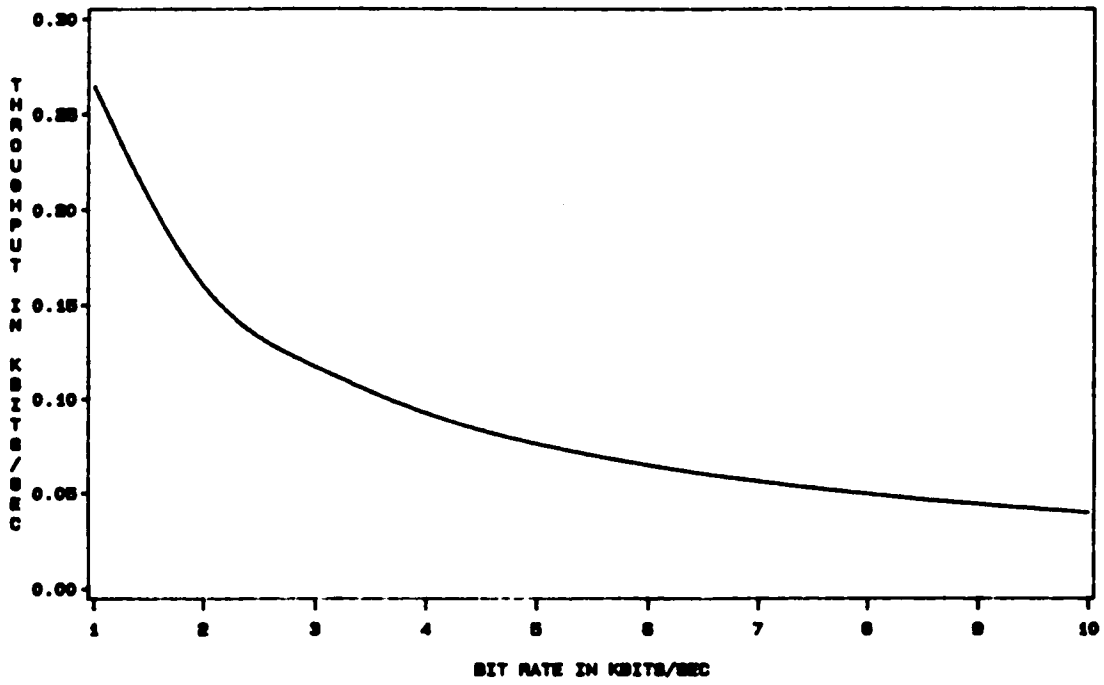

FIG. 10
AVERAGE THROUGHPUT RATE FOR AWGN CHANNEL
(UPPER BOUND)

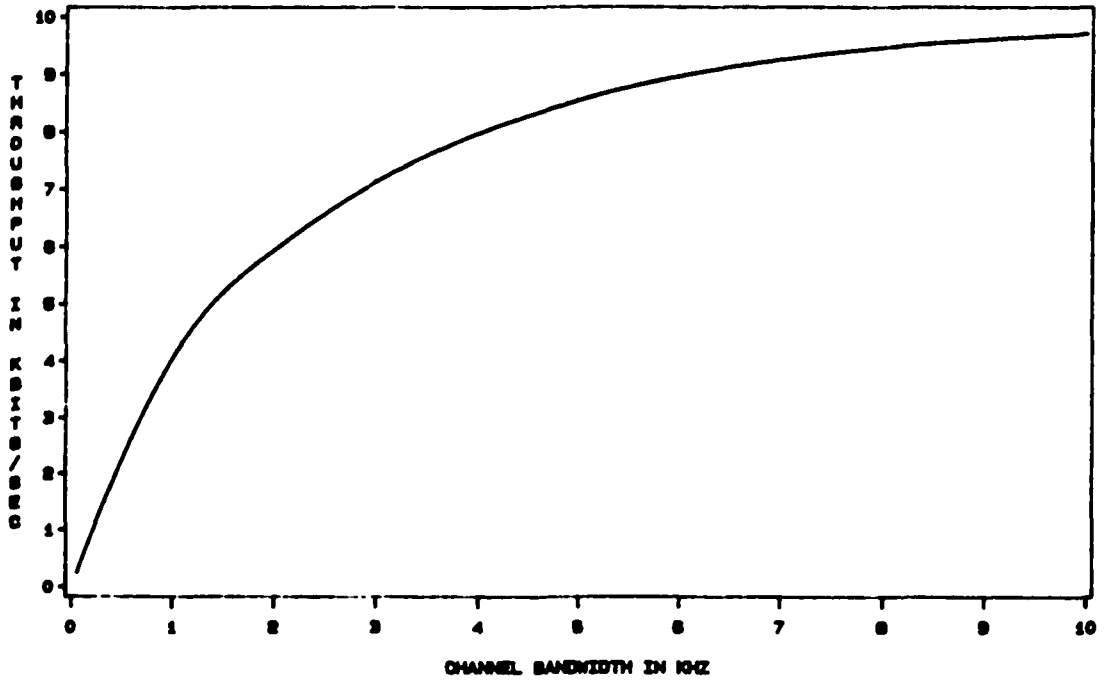

9. REFERENCES

[1] M.W. Abel, "Meteor Burst Communications: Bits per Burst Performance Bounds," IEEE Trans. Comm., vol. COM-34, Sep. 1986.

[2] J.B. Anderson, T. Aulin, and C.-E. Sundberg, Digital Phase Modulation, Plenum Press, New York and London, 1986.

[3] D.K. Bailey et al., "A New Kind of Radio Propagation at Very High Frequencies Observable over Long Distances," Phys. Rev., vol. 86, pp. 141-145, Apr. 1952.

[4] P.J. Bartholome and I.M. Vogt, "COMET - A New Meteor Burst System Incorporating ARQ and Diversity Reception," IEEE Trans. Commun. Technol., vol. COM-16, pp. 268-278, Apr. 1968.

[5] R.J. Benice and A.H. Frey, Jr., "An Analysis of Retransmission Systems," IEEE Trans. Commun. Technol., vol. COM-12, pp. 135-145, Dec. 1964.

[6] K. Brayer, "ARQ and Hybrid FEC-ARQ System Design to Meet Tight Performance Constraints," National Telecommunications Conference, Dallas, Texas, Nov. 1976.

[7] K. Brayer and S. Natarajan, "An Investigation of ARQ and FEC-ARQ on an Experimental High Latitude Meteor Burst Channel," Proc. of IEEE MILCOM '88, San Diego, CA, Oct. 1988.

[8] D.W. Brown, "Physical Meteor Burst Propagation Model and Some Significant Results for Communication System Design," IEEE J. Select. Areas Commun., vol. SAC-3, pp. 745-755, Sept. 1985.

[9] I.C. Browne and T.R. Kaiser, "The Radio Echo from the Head of Meteor Trails," J. Atmos. Terr. Phys., vol. 4, pp. 1-4, Sep. 1953.

[10] G. Clark and J. Cain, Error Correction Coding for Digital Communications, Plenum Press, New York, 1981.

[11] P.C. Crane, "An Empirical Analysis of the Application of Forward Error Correction to Meteor Burst Communication," Proc. of IEEE MILCOM '88, San Diego, CA, Oct. 1988.

[12] G.W.L. Davis, S.J. Gladys, G.R. Lang, L.M. Luke, and M.K. Taylor, "The Canadian JANET System," Proc. IRE, vol. 45, pp. 1666-1678, Dec. 1957.

[13] V.R. Eshleman and L.A. Manning, "Radio Communications by Scattering from Meteoric Ionization," Proc. IRE, vol. 42, pp. 530-537, Mar. 1954.

[14] V.R. Eshleman, "Theory of Radio Reflections from Electron-Ion Clouds," IRE Trans. Antennas Propag., vol. AP-3, pp. 32-39, Jan. 1955.

[15] V.R. Eshleman, "The Theoretical Length Distribution of Ionized Meteor Trails," J. Atmos. Terr. Phys., vol. 10, pp. 57-72, Feb. 1957.

[16] P.A. Forsyth, E.L. Vogan, D.R. Hansen, and C.O. Hines, "The Principles of JANET - A Meteor Burst Communication System," Proc. IRE, vol.45, pp. 1642-1657, Dec. 1957.

[17] I.S. Gradshteyn and I.M. Ryzhik, Table of Integrals, Series, and Products, Academic Press, Inc., Orlando, Florida, 1980.

[18] J.S. Greenhow and J.E. Hall, "The Importance of Initial Trail Radius on the Apparent Height and Number Distributions of Meteor Echoes," Monthly Notices Roy. Astron. Soc., vol. 121, pp 183-196, Aug. 1960.

[19] J.S. Greenhow and E.L. Neufeld, "The Diffusion of Ionized Meteor Trails in the Upper Atmosphere," J. Atmos. Terr. Phys., vol. 6, pp. 133-140, Mar. 1955.

[20] E.J. Haakinson, "Meteor Communications Model," Nat. Telecommun. Inform. Agency Rep. 83-116, U.S. Dept. Commerce, 1982.

[21] G.S. Hawkins, "A Radio Survey of Sporadic Meteor Radiants," Monthly Notices Roy. Astron. Soc., vol. 116, pp. 92-104, Nov. 1956.

[22] G.S. Hawkins and F.I. Whipple, "The Width of Meteor Trails," Astron. J., vol. 63, pp. 283-291, July 1958.

[23] J.A. Heller and I.W. Jacobs. "Viterbi Decoding for Satellite and Space Communication," IEEE Trans. Commun. Technol., vol COM-19, pp. 835-848, Oct. 1971.

[24] J.S. Hey and G.S. Stewart, "Derivation of Meteor Stream Radiants by Radio Reflexion Methods," Nature, vol. 158, pp. 481-482, Oct. 1946.

[25] E. Hibshoosh, "A Study of a Meteor Burst Communication System," Ph.D. Dissertation, City College of the City University of New York, New York, June 1987.

[26] C.O. Hines, "Diurnal Variations in Forward-Scattered Meteor Signals," J. Atmos. Terr. Phys., vol. 9, pp. 229-232, Oct. 1956.

[27] C.O. Hines and R.E. Pugh, "The Spatial Distribution of Signal Sources in Meteoric Forward Scattering," Can. J. Phys., vol. 34, pp. 1005-1015, Oct. 1956.

[28] IMSL Library - Reference Manual, IMSL, Inc., Houston, Texas, 1982.

[29] T.R. Kaiser, "Radio Echo Studies of Meteor Ionization," Advan. Phys., vol. 2, pp. 495-544, Oct. 1953.

[30] S. Lin and D.J. Costello, Error Control Coding - Fundamentals and Applications, Prentice Hall, Englewood Cliffs, New Jersey, 1983.

[31] L.A. Maynard, "Propagation of Meteor Burst Signals During the Polar Disturbance of November 12-16, 1960" Canad. J. Phys., vol. 39, pp. 628-629, Apr. 1964.

[32] D.W.R. McKinley, "Meteor Velocities Determined by Radio Observations," Astrophys. J., vol. 113, pp. 225-267, Mar. 1951.

[33] L.A. Manning, "Air Motions at Meteoric Heights," J. Atmos. Terr. Phys., vol. 15, pp. 137-140, Sep. 1959.

[34] L.A. Manning and V.R. Eshleman, "Meteors in the Ionosphere," Proc. IRE, vol. 47, pp. 186-199, Feb. 1959.

[35] A. Michelson and A. Levesque, Error Control Techniques for Digital Communications, John Wiley & Sons, New York, 1985.

[36] L.B. Milstein, D.L. Schilling, R.L. Pickholtz, J. Sellman, S. Davidovici, A. Pavelchek, A. Schneider, and G. Eichmann, "Performance of Meteor-Burst Communication Channels," IEEE J. Sel. Areas Commun., vol. SAC-5, pp. 146-154, Feb. 1987.

[37] G.F. Montgomery and G.R. Sugar, "The Utility of Meteor Bursts for Intermittent Radio Communication," Proc. IRE, vol. 45, pp. 1684-1693, Dec. 1957.

[38] J.M. Morris, "Optimal Blocklengths for ARQ Error Control Schemes," IEEE Trans. Comm., vol. COM-27, pp. 488-493, Feb. 1979.

[39] H. Nes, "Propagation Characteristics of Meteor-Burst Communication Systems," SHAPE Tech. Cen., The Hague, The Netherlands, Tech. Doc. STC TM-170, July 1983.

[40] J.P. Odenwalder, Error Control Coding Handbook, Linkabit Corp., San Diego, Calif., 1976.

[41] J.D. Oetting, "An Analysis of Meteor Burst Communications for Military Applications," J. Select. Areas. Commun., vol. COM-28, pp.1591-1601, Sep. 1980.

[42] A. Papoulis, Probability, Random Variables and Stochastic Processes, McGraw-Hill Book Company, New York, 1984.

[43] G.W. Pickard, "A Note on the Relation of Meteor Showers and Radio Reception," Proc. IRE, vol. 19, pp. 1166-1170, July 1931.

[44] V.C. Pineo, "Off-Path Propagation at VHF," Proc. IRE, vol. 46, p. 922, May 1958.

[45] N.J. Rudie, "The Relative Distribution of Observable Meteor Trails in Forward Scatter Meteor Communications," Ph.D. dissertation, Montana State Univ., Bozeman, Aug. 1967.

[46] C.E. Shannon, "Two-way Communication Channels," Proc. 4th Berkeley Symp. Prob. and Stat., vol. 1, pp. 611-644, Univ. California Press, Berkeley, CA, 1961.

[47] M.K. Simon, J.K. Omura, R.A. Scholtz, and B.K. Levitt, Spread Spectrum Communications - Volume I, Computer Science Press, Rockville, MD, 1985.

[48] R.D. Sinnot, D.R. Place, W.I. Thompson, H. Sunkenberg, J.D. Killian, and G. Benhal, "Meteor Burst Communication with a Buried Antenna," presented at the MILCOM Conf., Boston, MA, Oct. 1985, paper 32.J.

[49] B. Sklar, Digital Communications - Fundamentals and Applications, Prentice Hall, Englewood Cliffs, 1988.

[50] G.R. Sugar, "Radio Propagation by Reflection from Meteor Trails," Proc. IEEE, vol. 52, pp.117-136, Feb. 1964.

[51] H. Taub and D.L. Schilling, Principles of Communication Systems, 2nd edition, McGraw-Hill Book Company, New York, 1986.

[52] W.I. Thompson, J.R. Herman, and D.R. Place, "Results of Meteor Burst Communication with a Buried Antenna," in Proc. MILCOM Conf., Oct. 1986, paper 16.5.

[53] United States Armed Forces, Handbook of Geophysics, The Macmillan Company, New York, N.Y., 1960.

[54] A.J. Viterbi and J.K. Omura, Principles of Digital Communication and Coding, McGraw-Hill Book Company, New York, 1979.

[55] J.A. Weitzen, W.P. Birkemeier, and M.D. Grossi, "An Estimate of the Capacity of the Meteor Burst Channel," IEEE Trans. Commun., vol. COM-32, pp. 972-974, Aug. 1984.

[56] J.A. Weitzen and W. Nelson, "An Improved Model for Predicting the Occurrence of Meteors in Meteor Burst Communication," presented at the MILCOM Conf., Boston, MA, Oct. 1985, paper 32.4.

[57] J.A. Weitzen, "Predicting the Arrival of Meteors Useful for Meteor Burst Communication," Radio Sci., pp. 1009-1020, Nov. 1986.

[58] J.A. Weitzen, "A Data Base Approach to Analysis of Meteor Burst Data," Radio Sci., vol. 22, pp. 133-140, Jan. 1987.

[59] E.J. Weldon, "An Improved Selective-Repeat ARQ Strategy," IEEE Trans. Comm., vol. COM-30, pp. 480-486, Mar. 1982.

[60] J.M. Wozencraft and I.M. Jacobs, Principles of Communication Engineering, John Wiley & Sons, New York, 1965.